Eur. Phys. J. Plus (2018) **133**: 1
DOI 10.1140/epjp/i2018-11804-8

THE EUROPEAN PHYSICAL JOURNAL PLUS

Regular Article

Motion through a non-homogeneous porous medium: Hydrodynamic permeability of a membrane composed of cylindrical particles

Pramod Kumar Yadav[a]

Department of Mathematics, Motilal Nehru National Institute of Technology Allahabad, Allahabad, 211004 (U.P.), India

Received: 16 October 2017 / Revised: 21 November 2017
Published online: 5 January 2018 –

Abstract. The present problem is concerned with the flow of a viscous steady incompressible fluid through a non-homogeneous porous medium. Here, the non-homogeneous porous medium is a membrane built up by cylindrical particles. The flow outside the membrane is governed by the Stokes equation and the flow through the non-homogeneous porous membrane composed by cylindrical particles is governed by Darcy's law. In this work, we discussed the effect of various fluid parameters like permeability parameter k_0, discontinuity coefficient at fluid-non homogeneous porous interface, viscosity ratio of viscous incompressible fluid region and non-homogeneous porous region, etc. on hydrodynamic permeability of a membrane, stress and on velocity profile. The comparative study for hydrodynamic permeability of membrane built up by non-homogeneous porous cylindrical particles and porous cylindrical shell enclosing a cylindrical cavity has been studied. The effects of various fluid parameters on the streamlines flow patterns are also discussed.

1 Introduction

The flow of a viscous fluid through porous media has received considerable attention by the number of researchers because of its numerous applications in sedimentation, colloidal science, etc. In nature, such flows occur in cases of water formation, instruction of sea water to the coastal area and dams, flows to wells from water bearing formation and the flow of river water through the porous banks and thus land erosion. The most appropriate example of a non-homogenous multiphasic porous system is soil. Thus the flow of viscous incompressible fluid through the porous region plays an imperative role in the area of soil engineering. A major application of flow through porous media is blood flow through human arteries. The researches concerning the problems related to applications of Stokes equations, Darcy's equation and Brinkman equations in physical and biological sciences were carried out during the last previous years. A number of mathematical models, including an evaluation of a hydrodynamic permeability of different type membranes regarded as conglomerates of incompletely porous spherical particles and influence of porous coating on the flow rate through cylindrical capillaries have been generated by the researchers.

Stokes [1] discussed the theories of internal friction of viscous fluids when they are in motion, and of the equilibrium and motion of elastic bodies. Stokes equations can be used to study problems such as locomotion of micro-organism, flow of mucus in lungs and movement of minuscule particles having slow motion, small linear dimensions or high viscosity. Darcy [2] has investigated the flow of water in vertical homogeneous sand filters. He concludes that the rate of flow through porous media of low permeability is proportional to pressure drop, which is one of the basic models that have been used extensively in the literature. The flow of a viscous, steady, incompressible fluid through a porous spherical particle with the help of Darcy's law was discussed by Joseph and Tao [3]. With this discussion, they concluded that the drag on the porous sphere is same as that of solid sphere with reduced radius. However, this law is not applicable for the flow of a viscous, steady, incompressible fluid through porous region with high porosity, for flows in the neighbourhood of the surface of the bounded porous medium and large shear rates.

[a] e-mail: pramod547@gmail.com

Many early authors, *e.g.*, Neild and Bejan [4] have used various types of extended Darcy models for flow through porous media. The problem of the flow of a Newtonian fluid through porous media was studied by Preziosi and Farina [5] by using Darcy's law. The slip boundary condition at a naturally permeable wall was discussed by Beavers and Joseph [6]. The low Reynolds number flow of a viscous, incompressible fluid through porous spherical shell enclosing a cavity immersed in viscous fluid was investigated by Jones [7]. The creeping flow of a viscous, incompressible fluid through the composite sphere enclosed by a porous layer was studied by Masliyah *et al.* [8]. An exact solution for the creeping flow past a porous spherical shell was investigated by Qin and Kaloni [9]. The drag force experienced by a porous spherical shell was also evaluated by them. The problem of the steady two-dimensional Stokes flow stirred by an infinitesimal rotating cylinder in the annular region between two fixed concentric cylindrical walls was tackled by Hackborn [10]. The drag force exerted by the fluid on the porous cylinders in a viscous fluid at low Reynolds number was obtained by Stechkina [11]. The flow of a viscous steady incompressible fluid through a circular cylinder embedded in another medium with constant porosity was discussed by Pop and Cheng [12]. In this work, they showed that the separation of the fluid flow does not take place at the surface of the cylinder. The uniform flow of a steady, viscous, incompressible fluid through an inhomogeneous permeable circular cylinder by using Darcy's law was considered by Singh and Gupta [13].

Recently, Deo [14] has discussed the Stokes flow through a swarm of porous cylinders with Happel and Kuwabara boundary conditions. The problem of a fluid flow through a cylinder, when the fluid is viscoelastic was discussed by Ellero *et al.* [15] by using a numerical scheme based on smoothed particle hydrodynamics. In the membrane filtration process, the specific resistance of aggregated colloidal cake layers was evaluated by Kim and Yuan [16]. The comparative study for Happel, Kuwabara, Kvashnin and Cunningham/Mehta-Morse models when the quasisteady axisymmetric flow of an incompressible viscous fluid takes place in an axisymmetric porous spherical shell has been done by Saad [17]. The problem of two-dimensional Stokes flow through the permeable cylinders was considered by Palaniappan *et al.* [18]. The drag force exerted by fluid on a cylinder was discussed by Datta and Shukla [19] by using the slip boundary condition with a conclusion that the slippage on the cylinder reduces the drag force. The flow of viscous fluid through a porous circular cylinder, when the Reynolds number is small was considered by Verma and Bhatt [20]. In this problem, they discussed the effect of permeability and slip conditions which was discussed by Jones [7] on the flow through a porous cylinder. A theoretical derivation of Darcy's law was done by Whitaker [21] with the help of the volume averaging method by taking Stokes flow past a rigid porous region. The problem of flow of a steady viscous fluid through a circular cylinder was discussed by Mandujano and Peralta-Fabi [22]. In this work, they used the series truncation method to find the solutions to the problem. The flow of viscous, steady, incompressible fluid through the swarm of porous nanocylindrical particles enclosing a solid cylindrical core was discussed by Deo and Yadav [23].

The comparison of results for nonlinear fluid flow through porous media obtained by Quadratic and Power Law was discussed by Cheng *et al.* [24]. The flow of a viscous incompressible fluid through a membrane built up by porous cylindrical particles enclosing a solid core was studied by Deo *et al.* [25]. The flow of a steady, viscous, incompressible fluid through a swarm of porous particles with an impermeable core along the axis of a cylinder and perpendicular to the axis of a cylinder was discussed by Deo *et al.* [26]. The study of flow when a porous sphere is placed in an arbitrary oscillatory Stokes flow by using the Brinkman model was studied by Prakash and Raja Sekhar [27]. The problem of two-dimensional flow of incompressible gas with suspended particles in the flow around the porous cylinder under the assumption that particle concentration is low and the negligible influence of dispersed phase on the gas was discussed by Grigoreva and Zaripov [28]. The problem of a slow flow of viscous incompressible fluid through a deformed porous spheroid embedded in another porous medium has been discussed by Yadav and Deo [29] with the conclusion that the drag coefficient increases and the shearing stress decreases with the increase of permeability of the porous region. The slow flow of a viscous incompressible fluid through a porous cylindrical shell in a concentric cylindrical cavity was studied by Yadav [30]. Numerical modeling of two-dimensional fluid flow around and through a porous diamond-square cylinder was done by Valipour *et al.* [31]. The problem of the onset of convection in a vertical porous cylinder with the assumption that the lower and upper plane boundaries of the cylinder are impermeable walls was discussed by Barletta and Storesletten [32]. Srinivasan and Rajagopal [33] discussed the flow of fluids through inhomogeneous porous media due to high pressure gradients. The Cell models for viscous flow through a swarm of Reiner-Rivlin liquid spherical drops and for micropolar fluid through the viscous fluid sphere was discussed by Jaiswal and Gupta [34] and Saad [35] respectively. Chernyshev [36] studied the problem of the Stokes flow for a porous particle with radially non-uniform porosity.

Although a lot of work has been done on flow past a body with porous layer, in most of the above-mentioned works, it was found that the researchers have taken the homogeneous medium, *i.e.* lack of non-homogeneity of the porous region was observed. By considering the above fact in our mind, in this paper, we discussed the motion of a viscous, steady incompressible fluid through a non-homogenous porous membrane. The hydrodynamic drag force acting on non-homogeneous porous cylinder by the viscous, steady incompressible fluid and the hydrodynamic permeability of a membrane were evaluated. The influence of various parameters like permeability parameters of non-homogeneous porous media, viscosity ratio, particle volume fraction, etc., on the hydrodynamic drag force and hydrodynamic permeability of the membrane was discussed graphically.

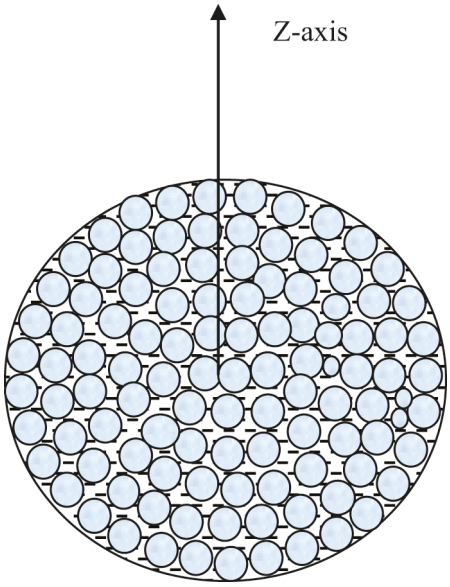

Fig. 1. The physical model.

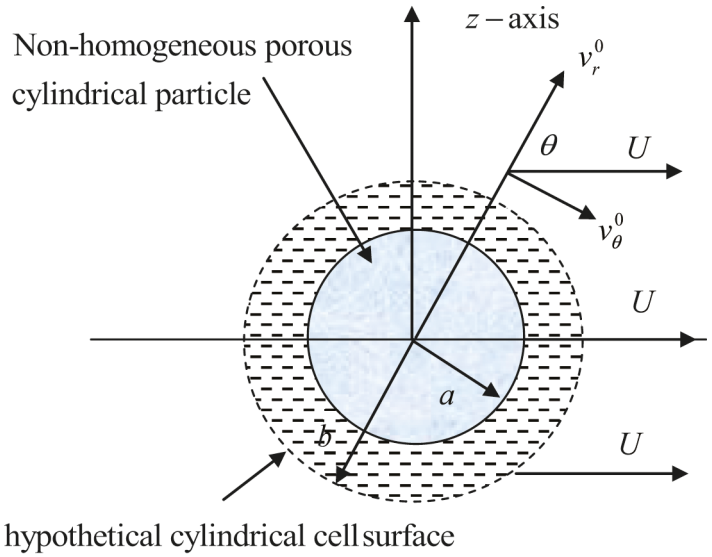

Fig. 2. Co-ordinate system.

2 Statement and mathematical formulation

In the present problem, we consider the motion of a viscous incompressible fluid through a non-homogenous porous medium which is in the form of a membrane and built up by non-homogenous porous cylindrical particles of radius $\tilde{a}$ (fig. 1). In a membrane, a system of co-axial non-homogenous porous cylinders of radii $\tilde{a}$ has been considered with their axes being parallel. Here, we assume that the membrane built up by non-homogenous porous cylindrical particles is also in the form of a cylinder. To know the hydrodynamic permeability of the membrane, we used the cell model technique. According to the cell model technique, we choose a single particle from the membrane and assume that each non-homogenous porous cylindrical particle is enveloped by a hypothetical cylindrical cell of radius $\tilde{b}$ (fig. 2).

Let us consider that the non-homogenous porous cylinder is stationary and the viscous incompressible fluid perpendicular to the axis of the cylinder (z-axis) with a uniform velocity $\tilde{\mathbf{U}}(|\tilde{\mathbf{U}}| = U)$ is approaching towards the cell and partially passing through the non-homogeneous porous cylinder. The slow flow of a Newtonian fluid with absolute viscosity is assumed as steady and axisymmetric. Let (r, θ, z) denote a cylindrical polar co-ordinate system with the origin on the axis of the cylinder of radius $\tilde{a}$ and the line of motion of the viscous incompressible fluid as an initial line.

Due to the axisymmetric flow, all the physical quantities are independent of z. Therefore, the velocity component $\tilde{v}_z$ vanishes along the z-direction. We shall denote i an entity for inside and o for outside regions of the non-homogenous porous cylinder, respectively.

The flow of the viscous, steady, incompressible fluid inside the non-homogenous porous region (*i.e.* $\tilde{r} \leq \tilde{a}$) is governed by Darcy's [2] equation together with the continuity equation

$$\tilde{\mu}^O \tilde{\mathbf{v}}^O = -K(\tilde{r})\tilde{\nabla}\tilde{p}^O, \tag{1}$$

$$\tilde{\nabla} \cdot \tilde{\mathbf{v}}^O = 0. \tag{2}$$

The flow of the viscous, steady, incompressible fluid outside the non-homogenous porous region ($\tilde{a} \leq \tilde{r} \leq \tilde{b}$) is governed by the Stokes equation (Happel and Brenner [37]) with continuity condition:

$$\tilde{\nabla}\tilde{p}^i = \tilde{\mu}^i \tilde{\Delta}\tilde{\mathbf{v}}^i, \tag{3}$$

$$\tilde{\nabla} \cdot \tilde{\mathbf{v}}^i = 0, \tag{4}$$

where the symbols $\sim$, above the variables mark dimensional values; $\tilde{K}(r)$ being the permeability coefficient of the non-homogeneous porous region which can be assumed as $k_0\tilde{r}^2$, $\tilde{\mathbf{v}}^o$, $\tilde{\mathbf{v}}^i$ are velocity outside and inside the porous region; $\tilde{p}^o$, $\tilde{p}^i$ are pressure outside and inside the porous region; $\tilde{\mu}^o$ and $\tilde{\mu}^i$ are viscosities of the fluid region and the effective viscosity of the non-homogeneous porous region. The relation between $\tilde{\mu}^o$ and $\tilde{\mu}^i$ will depend on the type of porous media, *i.e.* $\tilde{\mu}^o$ may be either greater or smaller than $\tilde{\mu}^i$.

3 Solution of the problem

Let us define the following non-dimensional variables to make the governing equation in dimensionless form:

$$\frac{1}{\gamma} = \frac{\tilde{b}}{\tilde{a}}, \qquad r = \frac{\tilde{r}}{\tilde{a}}, \qquad \nabla = \tilde{a}\tilde{\nabla}, \qquad \Delta = \tilde{\Delta} \cdot \tilde{a}^2, \qquad p = \frac{\tilde{p}}{\tilde{p}_o}, \qquad \tilde{p}_o = \frac{\tilde{U}\tilde{\mu}^o}{\tilde{a}},$$
$$\lambda^2 = \frac{\tilde{\mu}^o}{\tilde{\mu}^i}, \qquad v = \frac{\tilde{\mathbf{v}}}{\tilde{U}}, \qquad K(r) = \frac{\tilde{K}(r)}{\tilde{a}^2}, \qquad \text{and} \qquad \psi^{o,i} = \frac{\tilde{\psi}^{o,i}}{\tilde{U}\tilde{a}^2}. \tag{5}$$

Now using the relation (5), we can reduce the equations of flow (1)–(4) into non-dimensional form as follows.

For inside the non-homogeneous porous region:

$$\tilde{\mathbf{v}}^i = -\frac{\tilde{K}(r)}{\tilde{\mu}^i}\tilde{\nabla}\tilde{p}^i \Rightarrow \mathbf{v}^i\tilde{U} = -\frac{K(r)\tilde{a}^2}{\tilde{\mu}^i}\frac{\nabla}{\tilde{a}}p^i\tilde{p}_o \Rightarrow \mathbf{v}^i\tilde{U} = -\frac{K(r)\tilde{a}}{\tilde{\mu}^i}\tilde{p}_o\nabla p^i$$
$$\Rightarrow \mathbf{v}^i\tilde{U} = -\frac{K(r)\tilde{a}}{\tilde{\mu}^i}\frac{\tilde{U}\tilde{\mu}^o}{\tilde{a}}\nabla p^i \Rightarrow \mathbf{v}^i = -\lambda^2 K(r)\nabla p^i, \tag{6}$$

$$\tilde{\nabla} \cdot \tilde{\mathbf{v}}^i = 0 \Rightarrow \frac{1}{\tilde{a}^2}\nabla \cdot \mathbf{v}^i\tilde{U} = 0 \Rightarrow \frac{\tilde{U}}{\tilde{a}^2}\nabla \cdot \mathbf{v}^i = 0 \Rightarrow \nabla \cdot \mathbf{v}^i = 0. \tag{7}$$

For outside the non-homogeneous porous region:

$$\tilde{\nabla}\tilde{p}^o = \tilde{\mu}^o\tilde{\Delta}\tilde{\mathbf{v}}^o \Rightarrow \frac{\nabla}{\tilde{a}}p^o\tilde{p}_o = \tilde{\mu}^o\frac{\Delta}{\tilde{a}^2}\mathbf{v}^o\tilde{U} \Rightarrow \frac{\nabla}{\tilde{a}}p^o\frac{\tilde{U}}{\tilde{a}}\tilde{\mu}^o = \tilde{\mu}^o\frac{\Delta}{\tilde{a}^2}\mathbf{v}^o\tilde{U}, \qquad \Rightarrow \nabla p^o = \Delta\mathbf{v}^o. \tag{8}$$

Similarly, the non-dimensional form of the continuity equation for outside the non-homogeneous porous region can be written as

$$\nabla \cdot \mathbf{v}^o = 0. \tag{9}$$

Thus the system of governing equations (eqs. (1)–(4)) in dimensionless form can be written as:

$$\begin{cases} \nabla p^o = \Delta v^o, \\ \nabla \cdot v^o = 0, \end{cases} \qquad \left(1 \leq r \leq \frac{1}{\gamma}\right), \tag{10}$$

$$\begin{cases} \mathbf{v}^i = -\lambda^2 K(r)\nabla p^i, \\ \nabla \cdot v^i = 0, \end{cases} \qquad (r \leq 1). \tag{11}$$

Taking divergence of both sides of the first equation of eq. (11), we have

$$\nabla \cdot \mathbf{v}^i = -\lambda^2 \nabla(K(r)) \cdot (\nabla p^i) - \lambda^2 K(r)(\nabla \cdot \nabla p^i). \tag{12}$$

Using the second equation of eq. (11), we have

$$0 = \operatorname{grad} k(r) \cdot \operatorname{grad} p^i + K(r)\nabla^2 p^i \Rightarrow \frac{\partial K(r)}{\partial r}\frac{\partial p^i}{\partial r} + K(r)\left(\frac{\partial^2 p^i}{\partial r^2} + \frac{1}{r}\frac{\partial p^i}{\partial r} + \frac{1}{r^2}\frac{\partial^2 p^i}{\partial \theta^2}\right) = 0. \tag{13}$$

By the method of variable and separable, we can obtain the solution of eq. (13).

Let us assume that

$$p^i = g(r)\cos\theta. \tag{14}$$

By using power's law of porosity, we can also assume the variable porosity of material as

$$K(r) = k_o r^2, \quad k_o > 0. \tag{15}$$

Using eqs. (14) and (15) in eq. (13), we can get a second-order homogeneous partial differential equation:

$$r^2\frac{\partial^2 g(r)}{\partial r^2} + 3r\frac{\partial g(r)}{\partial r} - g(r) = 0. \tag{16}$$

Solving eq. (16), we have

$$g(r) = A_1 r^{-1+\sqrt{2}} + A_2 r^{-1-\sqrt{2}}. \tag{17}$$

Therefore, the suitable solution of eq. (16) for the flow inside the non-homogeneous porous cylinder will be (the constant A_2 will be zero because of singularity inside the non-homogeneous porous cylinder)

$$g(r) = A_1 r^{-1+\sqrt{2}}. \tag{18}$$

Thus, the pressure inside the non-homogeneous porous cylinder will be

$$p^i = A_1 r^{-1+\sqrt{2}}\cos\theta. \tag{19}$$

Hence, the components of velocity of the viscous, steady, incompressible fluid in the non-homogeneous porous medium will come out as follows:

$$v_r^i = -\lambda^2 k_o A_1\left(-1+\sqrt{2}\right) r^{\sqrt{2}}\cos\theta, \tag{20}$$

$$v_\theta^i = \lambda^2 k_o A_1 r^{\sqrt{2}}\sin\theta. \tag{21}$$

The stream function $\psi(r,\theta)$ for outside and inside the non-homogeneous porous cylinder may be defined as

$$\mathbf{v}_r^i = \frac{1}{r}\frac{\partial \psi^i}{\partial \theta}, \qquad \mathbf{v}_\theta^i = -\frac{\partial \psi^i}{\partial r}, \tag{22}$$

$$\mathbf{v}_r^o = \frac{1}{r}\frac{\partial \psi^o}{\partial \theta}, \qquad \mathbf{v}_\theta^o = -\frac{\partial \psi^o}{\partial r}. \tag{23}$$

By using the relation (22) and eqs. (20), (21), the stream function formulation for the flow inside the non-homogeneous porous cylinder will comes out as

$$\psi^i(r,\theta) = -\lambda^2 k_o A_1\left(-1+\sqrt{2}\right) r^{1+\sqrt{2}}\sin\theta. \tag{24}$$

Now, taking curl of first equation of eq. (10) and using the velocities-stream function relation (23) we get the fourth-order partial differential equation for the flow outside the non-homogeneous porous cylinder as follows:

$$\nabla^4 \psi^o = \nabla^2(\nabla^2 \psi^o) = 0, \tag{25}$$

where ∇^2 is an operator and given as

$$\nabla^2 = \frac{\partial^2}{\partial r^2} + \frac{1}{r}\frac{\partial}{\partial r} + \frac{1}{r^2}\frac{\partial^2}{\partial \theta^2}. \tag{26}$$

A suitable stream function solution of the Stokes equation (25) can be written as

$$\psi^o(r,\theta) = [B_1 r + B_2 r^3 + B_3/r + B_4 r \ln r] \sin\theta. \tag{27}$$

Using eq. (27) in eq. (23), the components of velocity of viscous, steady, incompressible fluid in cylindrical container outside the non-homogeneous porous cylinder can be obtained which is given as follows:

$$v_r^o(r,\theta) = [B_1 + B_2 r^2 + B_3/r^2 + B_4 \ln r] \cos\theta, \tag{28}$$

$$v_\theta^o(r,\theta) = -[B_1 + 3B_2 r^2 - B_3/r^2 + B_4(1 + \ln r)] \sin\theta. \tag{29}$$

Further, we have mathematical expression for tangential and normal stresses for outside and inside the non-homogeneous porous cylinder as follows:

$$\tau_{r\theta}^o = \lambda^2 \left[\frac{1}{r^2} \frac{\partial^2 \psi^o}{\partial \theta^2} + \frac{1}{r} \frac{\partial \psi^o}{\partial r} - \frac{\partial^2 \psi^o}{\partial r^2} \right], \tag{30}$$

$$\tau_{rr}^o = -p^o + \frac{2\lambda^2}{r} \left[\frac{\partial^2 \psi^o}{\partial r \partial \theta} - \frac{1}{r} \frac{\partial \psi^o}{\partial \theta} \right], \tag{31}$$

$$\tau_{r\theta}^i = \left[\frac{1}{r^2} \frac{\partial^2 \psi^i}{\partial \theta^2} + \frac{1}{r} \frac{\partial \psi^i}{\partial r} - \frac{\partial^2 \psi^i}{\partial r^2} \right], \tag{32}$$

$$\tau_{rr}^i = -p^i + \frac{2}{r} \left[\frac{\partial^2 \psi^i}{\partial r \partial \theta} - \frac{1}{r} \frac{\partial \psi^i}{\partial \theta} \right], \tag{33}$$

where the pressure outside the non-homogeneous porous cylinder may be obtained with the help of the following relations

$$\frac{\partial p^o}{\partial r} = \lambda^2 \left[\nabla^2 v_r^o - \frac{v_\theta^o}{r^2} - \frac{2}{r^2} \frac{\partial v_\theta^o}{\partial \theta} \right], \tag{34}$$

$$\frac{1}{r} \frac{\partial p^o}{\partial r} = \lambda^2 \left[\nabla^2 v_\theta^o - \frac{v_\theta^o}{r^2} + \frac{2}{r^2} \frac{\partial v_r^o}{\partial \theta} \right]. \tag{35}$$

By using the appropriate velocities in eqs. (30)–(35), we can obtain the stresses in both regions and pressure outside the non-homogeneous porous layer, respectively, as

$$\tau_{r\theta}^o = -4\lambda^2 \left(r B_2 + \frac{1}{r^3} B_3 \right) \sin\theta, \tag{36}$$

$$\tau_{rr}^o = -4\lambda^2 \left[r B_2 + \frac{1}{r^3} B_3 - \frac{1}{r} B_4 \right] \cos\theta, \tag{37}$$

$$\tau_{r\theta}^i = 2\left(-1 + \sqrt{2}\right) r^{-1+\sqrt{2}} \lambda^2 k_o A_1 \sin\theta, \tag{38}$$

$$\tau_{rr}^i = -r^{-1+\sqrt{2}} \left(-1 + 2\left(-2 + \sqrt{2}\right) \lambda^2 k_o \right) A_1 \cos\theta, \tag{39}$$

$$p^o = 2\lambda^2 \left[4 B_2 r - \frac{1}{r} B_4 \right] \cos\theta. \tag{40}$$

3.1 Boundary conditions and determination of arbitrary constants

In order to find the complete solution of the boundary value problems (1) and (3), we need suitable boundary conditions at non-homogeneous porous-fluid interfaces and on the hypothetical cell surface. The boundary conditions at the mentioned surfaces, which are physically realistic and mathematically consistent for this problem, can be taken as

At non-homogeneous porous-fluid interfaces, *i.e.* at $r = 1$

The pressure in a non-homogeneous porous region is equal to normal stress in fluid Chernyshev [36], *i.e.*

$$p^i = -p^o + 2\lambda^2 \frac{\partial v_r^o}{\partial r}. \tag{41}$$

The normal components of velocity in a non-homogeneous porous region are equal to the normal components of velocity in the outside region of non-homogeneous porous medium Masliyah [8], *i.e.*

$$v_r^i = v_r^o. \tag{42}$$

The tangential components of velocities outside and inside the non-homogeneous porous region have discontinuity and are proportional to the derivative of the tangential component of velocity in the outside of the non-homogeneous porous region with respect to the outward normal Pop and Cheng [12], *i.e.*

$$v_\theta^o - v_\theta^i = \beta\sqrt{k(r)}\frac{\partial v_\theta^o}{\partial r}\,, \tag{43}$$

where β is the dimensionless constant and this constant depends on the physical nature of the porous material and the geometry of its surface. For very small values of permeability coefficient on the surface, β varies from 0.25 to 10 (Masliyah [8], Pop and Cheng [12]).

At the surface of a hypothetical cell, *i.e.* at $r = \frac{1}{\gamma}$

The condition of uniform velocity at the hypothetical cell surface is

$$v_r^o = \cos\theta. \tag{44}$$

According to Happel's model:

$$\tau_{r\theta}^o(m,\theta) = 0. \tag{45a}$$

According to Kuwabara's model:

$$\nabla^2\psi^o(m,\theta) = 0. \tag{45b}$$

According to Kvashnin's model:

$$\frac{\partial v_\theta^o}{\partial r} = 0. \tag{45c}$$

According to Mehta-Morse's model:

$$v_\theta^o = -\sin\theta. \tag{45d}$$

Using eqs. (19)–(21), (28), (29) and (40) in eqs. (41)–(45), we have

$$4\lambda^2 B_2 + 4\lambda^2 B_3 - 4\lambda^2 B_4 + A_1 = 0, \tag{46}$$

$$-B_1 - B_2 - B_3 - \left(-1+\sqrt{2}\right)\lambda^2 k_0 A_1 = 0, \tag{47}$$

$$B_1 + \left(3 - 6\beta\sqrt{k_0}\right)B_2 - \left(1 + 2\beta\sqrt{k_0}\right)B_3 + \left(1 - \beta\sqrt{k_0}\right)B_4 + \lambda^2 k_0 A_1 = 0, \tag{48}$$

$$\gamma^2 B_1 + B_2 + \gamma^4 B_3 + \gamma^2 \ln\left(\frac{1}{\gamma}\right)B_4 = \gamma^2, \tag{49}$$

$$B_2 + \gamma^4 B_3 = 0, \tag{50a}$$

$$4B_2 + \gamma^2 B_4 = 0, \tag{50b}$$

$$6B_2 + 2\gamma^4 B_3 + \gamma^2 B_4 = 0, \tag{50c}$$

$$\gamma^2 B_1 + 3B_2 - \gamma^4 B_3 + \gamma^2\left(1 + \ln\left(\frac{1}{\gamma}\right)\right)B_4 = \gamma^2. \tag{50d}$$

Solving the system of eqs. (46)–(49) together with one of eqs. (50), *i.e.* for Happel's model, Kuwabara's model, Kvashnin's model and Mehta-Morse's model, respectively, we can evaluate the arbitrary constants B_1, B_2, B_3, B_4 and A_1 for all the models, respectively. Therefore the stream function formulation for both the regions has been determined completely for all the models.

4 Hydrodynamic permeability and stresses

4.1 Evaluation of the drag force

The hydrodynamic drag force $\tilde{F}$ experienced by a non-homogeneous porous cylinder in a cylindrical container from the side of a liquid is defined as

$$\tilde{F} = \int_0^{2\pi} (\tau_{rr}^o \cos\theta - \tau_{r\theta}^o \sin\theta)_{r=1} \tilde{a} \mathrm{d}\theta. \tag{51}$$

Integrating the normal and tangential stresses (eqs. (37) and (36)) over the non-homogeneous porous cylindrical particle, we can obtain the experienced hydrodynamic drag force F which is given as

$$\tilde{F} = 4\pi\lambda^2 \tilde{a}\tilde{U} B_4. \tag{52}$$

Hence, the drag force F for all models, respectively, will come as follows.

Happel's model:

$$F = \tilde{a}\tilde{U}\left[8\pi\lambda^2\left(-1-\gamma^4+\beta(-1+3\gamma^4)\sqrt{k_0}+2\left(-2+\sqrt{2}\right)(-1+\gamma^4)\lambda^4 k_0\right)\right] \Big/ \left[1-\gamma^4-2(1+\gamma^4)\,\mathrm{Log}\left(\frac{1}{\gamma}\right)+\beta\left(-1+\gamma^4+(-2+6\gamma^4)\,\mathrm{Log}\left(\frac{1}{\gamma}\right)\right)\sqrt{k_0}+4\lambda^4\Big(-1+\left(5-4\sqrt{2}\right)\gamma^4 + \left(-2+\sqrt{2}\right)(-1+\gamma^4)\,\mathrm{Log}\left(\frac{1}{\gamma}\right)\Big)k_0+4\left(-1+\sqrt{2}\right)\beta(-3+7\gamma^4)\lambda^4 k_0^{3/2}\right]. \tag{53a}$$

Kuwabara's model:

$$F = -\tilde{a}\tilde{U}\left[16\pi\lambda^2\left(1+\beta\sqrt{k_0}+2\left(-2+\sqrt{2}\right)\lambda^4 k_0\right)\right] \Big/ \left[3-4\gamma^2+\gamma^4-4\,\mathrm{Log}\left[\frac{1}{\gamma}\right]-\beta\Big(1-4\gamma^2 + 3\gamma^4+4\,\mathrm{Log}\left[\frac{1}{\gamma}\right]\Big)\sqrt{k_0}-2\lambda^4\left(6-\sqrt{2}+4\left(-3+2\sqrt{2}\right)\gamma^2+\left(-2+\sqrt{2}\right)\gamma^4+4\left(-2+\sqrt{2}\right)\mathrm{Log}\left[\frac{1}{\gamma}\right]\right)k_0 + 8\left(-1+\sqrt{2}\right)\beta(-3+\gamma^2)\lambda^4 k_0^{3/2}\right]. \tag{53b}$$

Kvashnin's model:

$$F = \left(4\pi\lambda^2\left(-3-\gamma^4+3\beta(-1+\gamma^4)\sqrt{k_0}+2\left(-2+\sqrt{2}\right)(-3+\gamma^4)\lambda^4 k_0\right)\right) \Big/ \left(2-2\gamma^2-(3 + \gamma^4)\,\mathrm{Log}\left[\frac{1}{\gamma}\right]+\beta(-1+\gamma^2)\left(1-\gamma^2+3(1+\gamma^2)\,\mathrm{Log}\left[\frac{1}{\gamma}\right]\right)\sqrt{k_0}+\lambda^4\Big(-8+\sqrt{2}+\left(12-8\sqrt{2}\right)\gamma^2 + \left(12-9\sqrt{2}\right)\gamma^4+2\left(-2+\sqrt{2}\right)(-3+\gamma^4)\,\mathrm{Log}\left[\frac{1}{\gamma}\right]\Big)k_0+2\left(-1+\sqrt{2}\right)\beta\left(-9+2\gamma^2+7\gamma^4\right)\lambda^4 k_0^{3/2}\Big). \tag{53c}$$

Mehta-Morse's model:

$$\tilde{F} = \tilde{a}\tilde{U}\Big[\left(4\pi\lambda^2\left(-1+\gamma^4-(\beta+3\beta\gamma^4)\sqrt{k_0}+2\left(-2+\sqrt{2}\right)(1+\gamma^4)\lambda^4 k_0\right)\right) \Big/ \Big((-1+\gamma^2)\Big(-1+\gamma^2+(1+\gamma^2)\ln\left(\frac{1}{\gamma}\right)\Big)-\beta\left(2\gamma^2(-1+\gamma^2)+(1+3\gamma^4)\ln\left(\frac{1}{\gamma}\right)\right)\sqrt{k_0}+\lambda^4\Big(-(-1+\gamma^2)\left(4-\sqrt{2} + \left(-8+7\sqrt{2}\right)\gamma^2\right)+2\left(-2+\sqrt{2}\right)(1+\gamma^4)\ln\left(\frac{1}{\gamma}\right)\Big)k_0+2\left(-1+\sqrt{2}\right)\beta(3-2\gamma^2+7\gamma^4)\lambda^4 k_0^{3/2}\Big)\Big]. \tag{53d}$$

4.2 Evaluation of the dimensionless hydrodynamic permeability of the membrane

Hydrodynamic permeability of membrane $\tilde{L}_{11}$ built up by porous cylinder in a cylindrical container is defined as the ratio of uniform flow rate $\tilde{U}$ to the cell gradient pressure $\tilde{F}/\tilde{V}$ (Vasin *et al.* [38])

$$\tilde{L}_{11} = \frac{\tilde{U}}{\tilde{F}/\tilde{V}}\,, \tag{54}$$

where $\tilde{V} = \pi\tilde{b}^2$ is the volume of the cylindrical container of the unit length.

Using the value of $\tilde{F}$ from eq. (52) and the value of $\tilde{V}$ from above in eq. (54) we get

$$\tilde{L}_{11} = \frac{1}{4\lambda^2\gamma^2 B_4}\tilde{a} = L_{11}\tilde{a}, \tag{55}$$

where $L_{11} = \frac{1}{4\lambda^2\gamma^2 B_4}$ is the dimensionless hydrodynamic permeability of a membrane.

Substituting the value of B_4 in the above equation, we have the following.

Happel's model:

$$\begin{aligned} L_{11} = &\left[1-\gamma^4-2(1+\gamma^4)\,\mathrm{Log}\left[\frac{1}{\gamma}\right]+\beta\left(-1+\gamma^4+(-2+6\gamma^4)\,\mathrm{Log}\left[\frac{1}{\gamma}\right]\right)\sqrt{k_0}\right.\\ &+4\lambda^4\Big(-1+\left(5-4\sqrt{2}\right)\gamma^4+\left(-2+\sqrt{2}\right)(-1+\gamma^4)\,\mathrm{Log}\left[\frac{1}{\gamma}\right]\Big)k_0+4\left(-1+\sqrt{2}\right)\beta(-3+7\gamma^4)\lambda^4k_0^{\frac{3}{2}}\Big]\Big/\\ &\Big[8\gamma^2\lambda^2\Big(-1-\gamma^4+\beta(-1+3\gamma^4)\sqrt{k_0}+2\left(-2+\sqrt{2}\right)(-1+\gamma^4)\lambda^4k_0\Big)\Big]. \end{aligned} \tag{56a}$$

Kuwabara's model:

$$\begin{aligned} L_{11} = &\left[-3+4\gamma^2-\gamma^4+4\,\mathrm{Log}\left[\frac{1}{\gamma}\right]+\beta\left(1-4\gamma^2+3\gamma^4+4\,\mathrm{Log}\left[\frac{1}{\gamma}\right]\right)\sqrt{k_0}+2\lambda^4\Big(6-\sqrt{2}\right.\\ &+4\left(-3+2\sqrt{2}\right)\gamma^2+\left(-2+\sqrt{2}\right)\gamma^4+4\left(-2+\sqrt{2}\right)\mathrm{Log}\left[\frac{1}{\gamma}\right]\Big)k_0-8\left(-1+\sqrt{2}\right)\beta(-3+\gamma^2)\lambda^4k_0^{\frac{3}{2}}\Big]\Big/\\ &\left[16\gamma^2\lambda^2\left(1+\beta\sqrt{k_0}+2\left(-2+\sqrt{2}\right)\lambda^4k_0\right)\right]. \end{aligned} \tag{56b}$$

Kvashnin's model:

$$\begin{aligned} L_{11} = &\left(2-2\gamma^2-(3+\gamma^4)\,\mathrm{Log}\left[\frac{1}{\gamma}\right]+\beta(-1+\gamma^2)\left(1-\gamma^2+3(1+\gamma^2)\,\mathrm{Log}\left[\frac{1}{\gamma}\right]\right)\sqrt{k_0}+\lambda^4\Big(-8+\sqrt{2}\right.\\ &+4\left(3-2\sqrt{2}\right)\gamma^2+3\left(4-3\sqrt{2}\right)\gamma^4+2\left(-2+\sqrt{2}\right)(-3+\gamma^4)\,\mathrm{Log}\left[\frac{1}{\gamma}\right]\Big)k_0+2\left(-1+\sqrt{2}\right)\beta(-9+2\gamma^2\\ &\left.+7\gamma^4)\lambda^4k_0^{3/2}\right)\Big/\left(4\gamma^2\lambda^2\left(-3-\gamma^4+3\beta(-1+\gamma^4)\sqrt{k_0}+2\left(-2+\sqrt{2}\right)(-3+\gamma^4)\lambda^4k_0\right)\right). \end{aligned} \tag{56c}$$

Mehta-Morse's model:

$$\begin{aligned} L_{11} = &\left((-1+\gamma^2)^2+(-1+\gamma^4)\ln\left(\frac{1}{\gamma}\right)-\beta\left(2\gamma^2(-1+\gamma^2)+(1+3\gamma^4)\ln\left(\frac{1}{\gamma}\right)\right)\sqrt{k_0}+\lambda^4\Big(-(-1\right.\\ &+\gamma^2)\left(4-\sqrt{2}+\left(-8+7\sqrt{2}\right)\gamma^2\right)+2\left(-2+\sqrt{2}\right)(1+\gamma^4)\ln\left(\frac{1}{\gamma}\right)\Big)k_0+2\left(-1+\sqrt{2}\right)\beta(3-2\gamma^2\\ &\left.+7\gamma^4)\lambda^4k_0^{3/2}\right)\Big/\left(4\gamma^2\lambda^2\left(-1+\gamma^4-(\beta+3\beta\gamma^4)\sqrt{k_0}+2\left(-2+\sqrt{2}\right)(1+\gamma^4)\lambda^4k_0\right)\right). \end{aligned} \tag{56d}$$

When permeability k_o of the non-homogeneous porous region vanishes, then the above model behaves like a creeping flow of a viscous steady incompressible fluid through a membrane composed of impermeable cylinder of radius $\tilde{a}$. In this case, the value of the drag force experienced by the membrane and the dimensionless hydrodynamic permeability of a membrane comes out as follows.

Happel's model:

$$F = \frac{8\pi(1+\gamma^4)\lambda^2}{-1+\gamma^4+2(1+\gamma^4)\log(\frac{1}{\gamma})};$$
$$L_{11} = \frac{-1+\gamma^4+2(1+\gamma^4)\log(\frac{1}{\gamma})}{8\gamma^2(1+\gamma^4)\lambda^2}, \tag{57}$$

which agrees with the previously established results of Deo *et al.* [25].
Kuwabara's model:

$$F = -\frac{16\pi\lambda^2}{3-4\gamma^2+\gamma^4-4\log(\frac{1}{\gamma})};$$
$$L_{11} = -\frac{3-4\gamma^2+\gamma^4-4\log(\frac{1}{\gamma})}{16\gamma^2\lambda^2}. \tag{58}$$

This result agrees with the earlier result as reported by Deo *et al.* [23].
Kvashnin's model:

$$F = \frac{4\pi(3+\gamma^4)\lambda^2}{2(-1+\gamma^2)+(3+\gamma^4)\log(\frac{1}{\gamma})};$$
$$L_{11} = \frac{2(-1+\gamma^2)+(3+\gamma^4)\log(\frac{1}{\gamma})}{4\gamma^2(3+\gamma^4)\lambda^2}. \tag{59}$$

Mehta-Morse's model:

$$F = \frac{4\pi(1+\gamma^2)\lambda^2}{-1+\gamma^2+(1+\gamma^2)\log(\frac{1}{\gamma})};$$
$$L_{11} = \frac{-1+\gamma^2+(1+\gamma^2)\log(\frac{1}{\gamma})}{4\gamma^2(1+\gamma^2)\lambda^2}. \tag{60}$$

Results (59) and (60) agree with the earlier result as reported by Yadav [30].

4.3 Evaluation of the stresses inside and outside the non-homogeneous porous region

The stresses inside and outside the membrane for all models can be evaluated by using the value of appropriate constants in eqs. (36)–(39), which are as follows.

Happel's model:

$$\tau^o_{r\theta} = -\left[4\left(-1+r^4\gamma^4\right)\lambda^2\sin[\theta]\left(1-\beta\sqrt{k_0}+4\left(-2+\sqrt{2}\right)\lambda^4k_0\right)\right]\Big/\left[r^3\Big(1-\gamma^4-2(1+\gamma^4)\log\left(\frac{1}{\gamma}\right)+\beta\left(-1+\gamma^4+(-2+6\gamma^4)\log\left(\frac{1}{\gamma}\right)\right)\sqrt{k_0}+4\lambda^4\Big(-1+\left(5-4\sqrt{2}\right)\gamma^4+\left(-2+\sqrt{2}\right)(-1+\gamma^4)\log\left(\frac{1}{\gamma}\right)\Big)k_0+4\left(-1+\sqrt{2}\right)\beta(-3+7\gamma^4)\lambda^4k_0^{3/2}\Big)\right], \tag{61}$$

$$\tau^{i}_{r\theta} = -\left[8\left(-1+\sqrt{2}\right)r^{-1+\sqrt{2}}\lambda^4\sin[\theta]\left(-1-3\gamma^4+\beta(-3+7\gamma^4)\sqrt{k_0}\right)k_0\right]\Big/\Big[1-\gamma^4-2(1+\gamma^4)\log\left(\frac{1}{\gamma}\right)+\beta\left(-1+\gamma^4+(-2+6\gamma^4)\log\left(\frac{1}{\gamma}\right)\right)\sqrt{k_0}+4\lambda^4\Big(-1+\left(5-4\sqrt{2}\right)\gamma^4+\left(-2+\sqrt{2}\right)(-1+\gamma^4)\log\left(\frac{1}{\gamma}\right)\Big)k_0+4\left(-1+\sqrt{2}\right)\beta(-3+7\gamma^4)\lambda^4k_0^{3/2}\Big], \tag{62}$$

$$\tau^{o}_{rr} = -\Big[4\lambda^2\cos[\theta]\Big(-1+r^2\left(2+(2+r^2)\gamma^4\right)+\beta\left(1+r^2(2-(6+r^2)\gamma^4)\right)\sqrt{k_0}+4\Big(-2+\sqrt{2}\Big)\left(-1+r^2\right)\left(1+r^2\gamma^4\right)\lambda^4k_0\Big)\Big]\Big/\Big[r^3\Big(1-\gamma^4-2(1+\gamma^4)\log\left(\frac{1}{\gamma}\right)+\beta\Big(-1+\gamma^4+(-2+6\gamma^4)\log\left(\frac{1}{\gamma}\right)\Big)\sqrt{k_0}+4\lambda^4\left(-1+(5-4\sqrt{2})\gamma^4+\left(-2+\sqrt{2}\right)(-1+\gamma^4)\log\left(\frac{1}{\gamma}\right)\right)k_0+4\Big(-1+\sqrt{2}\Big)\beta(-3+7\gamma^4)\lambda^4k_0^{3/2}\Big)\Big], \tag{63}$$

$$\tau^{i}_{rr} = -\left[4r^{-1+\sqrt{2}}\lambda^2\cos[\theta]\left(-1-3\gamma^4+\beta(-3+7\gamma^4)\sqrt{k_0}\right)\left(-1+2\left(-2+\sqrt{2}\right)\lambda^2k_0\right)\right]\Big/\Big[1-\gamma^4-2(1+\gamma^4)\log\left(\frac{1}{\gamma}\right)+\beta\left(-1+\gamma^4+(-2+6\gamma^4)\log\left(\frac{1}{\gamma}\right)\right)\sqrt{k_0}+4\lambda^4\Big(-1+\left(5-4\sqrt{2}\right)\gamma^4+\Big(-2+\sqrt{2}\Big)(-1+\gamma^4)\log\left(\frac{1}{\gamma}\right)\Big)k_0+4\left(-1+\sqrt{2}\right)\beta(-3+7\gamma^4)\lambda^4k_0^{3/2}\Big]. \tag{64}$$

Kuwabara's model:

$$\tau^{o}_{r\theta} = \Big[4\lambda^2\sin[\theta]\Big(-2+(1+r^4)\gamma^2+\beta\left(2+(-3+r^4)\gamma^2\right)\sqrt{k_0}+2\left(-2+\sqrt{2}\right)(-4+(-1+r^4)\gamma^2)\lambda^4k_0\Big)\Big]\Big/\Big[r^3\Big(-3+4\gamma^2-\gamma^4+4\log\left(\frac{1}{\gamma}\right)+\beta\left(1-4\gamma^2+3\gamma^4+4\log\left(\frac{1}{\gamma}\right)\right)\sqrt{k_0}+2\lambda^4\Big(6-\sqrt{2}+4\left(-3+2\sqrt{2}\right)\gamma^2+\left(-2+\sqrt{2}\right)\gamma^4+4\left(-2+\sqrt{2}\right)\log\left(\frac{1}{\gamma}\right)\Big)k_0-8\left(-1+\sqrt{2}\right)\beta(-3+\gamma^2)\lambda^4k_0^{3/2}\Big)\Big], \tag{65}$$

$$\tau^{i}_{r\theta} = \left[16\left(-1+\sqrt{2}\right)r^{-1+\sqrt{2}}\lambda^4\sin[\theta]\left(-1-\gamma^2+\beta(-3+\gamma^2)\sqrt{k_0}\right)k_0\right]\Big/\Big[-3+4\gamma^2-\gamma^4+4\log\left(\frac{1}{\gamma}\right)+\beta\left(1-4\gamma^2+3\gamma^4+4\log\left(\frac{1}{\gamma}\right)\right)\sqrt{k_0}+2\lambda^4\Big(6-\sqrt{2}+4\left(-3+2\sqrt{2}\right)\gamma^2+\left(-2+\sqrt{2}\right)\gamma^4+4\left(-2+\sqrt{2}\right)\log\left(\frac{1}{\gamma}\right)\Big)k_0-8\left(-1+\sqrt{2}\right)\beta(-3+\gamma^2)\lambda^4k_0^{3/2}\Big], \tag{66}$$

$$\tau^{o}_{rr} = \Big[4\lambda^2\cos[\theta]\Big(-2+4r^2+\gamma^2+r^4\gamma^2+\beta(2+4r^2-3\gamma^2+r^4\gamma^2)\sqrt{k_0}+2\left(-2+\sqrt{2}\right)(-1+r^2)(4+(1+r^2)\gamma^2)\lambda^4k_0\Big)\Big]\Big/\Big[r^3\Big(-3+4\gamma^2-\gamma^4+4\log\left(\frac{1}{\gamma}\right)+\beta\left(1-4\gamma^2+3\gamma^4+4\log\left(\frac{1}{\gamma}\right)\right)\sqrt{k_0}+2\lambda^4\left(6-\sqrt{2}+4\left(-3+2\sqrt{2}\right)\gamma^2+\left(-2+\sqrt{2}\right)\gamma^4+4\left(-2+\sqrt{2}\right)\log\left(\frac{1}{\gamma}\right)\right)k_0-8\left(-1+\sqrt{2}\right)\beta(-3+\gamma^2)\lambda^4k_0^{3/2}\Big)\Big], \tag{67}$$

$$\tau^{i}_{rr} = \left[8r^{-1+\sqrt{2}}\lambda^2\cos[\theta]\left(-1-\gamma^2+\beta(-3+\gamma^2)\sqrt{k_0}\right)\left(-1+2\left(-2+\sqrt{2}\right)\lambda^2k_0\right)\right]\Big/\Big[-3+4\gamma^2-\gamma^4+4\log\left(\frac{1}{\gamma}\right)+\beta\left(1-4\gamma^2+3\gamma^4+4\log\left(\frac{1}{\gamma}\right)\right)\sqrt{k_0}+2\lambda^4\Big(6-\sqrt{2}+4\left(-3+2\sqrt{2}\right)\gamma^2+\Big(-2+\sqrt{2}\Big)\gamma^4+4\left(-2+\sqrt{2}\right)\log\left(\frac{1}{\gamma}\right)\Big)k_0-8\left(-1+\sqrt{2}\right)\beta(-3+\gamma^2)\lambda^4k_0^{3/2}\Big]. \tag{68}$$

Kvashnin's model:

$$\tau^{o}_{r\theta} = -\Bigg(\Big(2\lambda^2 \sin[\theta] \Big(-3+\gamma^2\left(1+r^4(1+\gamma^2)\right) - \beta(-1+\gamma)(1+\gamma)\left(3+r^4\gamma^2\right)\sqrt{k_0} + 2\Big(-2 + \sqrt{2}\Big)\left(-6+(-1+r^4)\gamma^2+2r^4\gamma^4\right)\lambda^4 k_0\Big)\Big) \Big/ \Bigg(r^3\left(2-2\gamma^2-(3+\gamma^4)\log\left(\frac{1}{\gamma}\right)+\beta(-1+\gamma^2)\Big(1-\gamma^2 + 3(1+\gamma^2)\log\left(\frac{1}{\gamma}\right)\Big)\sqrt{k_0} + \lambda^4\Big(-8+\sqrt{2}+4\left(3-2\sqrt{2}\right)\gamma^2+3\left(4-3\sqrt{2}\right)\gamma^4+2\left(-2+\sqrt{2}\right)(-3 + \gamma^4)\log\left(\frac{1}{\gamma}\right)\Big)k_0 + 2\left(-1+\sqrt{2}\right)\beta\left(-9+2\gamma^2+7\gamma^4\right)\lambda^4 k_0^{3/2}\Big)\Big)\Bigg), \tag{69}$$

$$\tau^{i}_{r\theta} = \Big(4\left(-1+\sqrt{2}\right)r^{-1+\sqrt{2}}\lambda^4\sin[\theta]\left(3+2\gamma^2+3\gamma^4+\beta(9-2\gamma^2-7\gamma^4)\sqrt{k_0}\right)k_0\Big) \Big/ \Big(2-2\gamma^2-(3 + \gamma^4)\log\left(\frac{1}{\gamma}\right)+\beta(-1+\gamma^2)\left(1-\gamma^2+3(1+\gamma^2)\log\left(\frac{1}{\gamma}\right)\right)\sqrt{k_0} + \lambda^4\Big(-8+\sqrt{2}+4\left(3-2\sqrt{2}\right)\gamma^2 + 3\left(4-3\sqrt{2}\right)\gamma^4+2\left(-2+\sqrt{2}\right)(-3+\gamma^4)\log\left(\frac{1}{\gamma}\right)\Big)k_0 + 2\left(-1+\sqrt{2}\right)\beta(-9+2\gamma^2+7\gamma^4)\lambda^4 k_0^{3/2}\Big), \tag{70}$$

$$\tau^{o}_{rr} = -\Bigg(\Big(2\lambda^2\cos[\theta]\Big(-3+\gamma^2+2r^2(3+\gamma^4)+r^4(\gamma^2+\gamma^4)-\beta(-1+\gamma^2)\Big(3+r^2\Big(6+(6 + r^2)\gamma^2\Big)\Big)\sqrt{k_0}+2\left(-2+\sqrt{2}\right)(-1+r^2)(6+(1+r^2)\gamma^2+2r^2\gamma^4)\lambda^4 k_0\Big)\Big) \Big/ \Bigg(r^3\Big(2-2\gamma^2-(3 + \gamma^4)\log\left(\frac{1}{\gamma}\right)+\beta(-1+\gamma^2)\left(1-\gamma^2+3(1+\gamma^2)\log\left(\frac{1}{\gamma}\right)\right)\sqrt{k_0} + \lambda^4\Big(-8+\sqrt{2}+4\left(3-2\sqrt{2}\right)\gamma^2 + 3\left(4-3\sqrt{2}\right)\gamma^4+2\left(-2+\sqrt{2}\right)(-3+\gamma^4)\log\left(\frac{1}{\gamma}\right)\Big)k_0 + 2\left(-1+\sqrt{2}\right)\beta(-9+2\gamma^2+7\gamma^4)\lambda^4 k_0^{3/2}\Big)\Big)\Bigg), \tag{71}$$

$$\tau^{i}_{rr} = \Big(2r^{-1+\sqrt{2}}\lambda^2\cos[\theta]\left(3+2\gamma^2+3\gamma^4+\beta(9-2\gamma^2-7\gamma^4)\sqrt{k_0}\right)\left(-1+2\left(-2+\sqrt{2}\right)\lambda^2 k_0\right)\Big) \Big/ \Big(2 - 2\gamma^2-(3+\gamma^4)\log\left(\frac{1}{\gamma}\right)+\beta(-1+\gamma^2)\left(1-\gamma^2+3(1+\gamma^2)\log\left(\frac{1}{\gamma}\right)\right)\sqrt{k_0} + \lambda^4\Big(-8+\sqrt{2}+4\Big(3 - 2\sqrt{2}\Big)\gamma^2+3\left(4-3\sqrt{2}\right)\gamma^4+2\left(-2+\sqrt{2}\right)(-3+\gamma^4)\log\left(\frac{1}{\gamma}\right)\Big)k_0 + 2\left(-1+\sqrt{2}\right)\beta(-9+2\gamma^2+7\gamma^4)\lambda^4 k_0^{3/2}\Big). \tag{72}$$

Mehta-Morse's model:

$$\tau^{o}_{r\theta} = -\Bigg(\Big(2\lambda^2 \sin[\theta]\Big((-1+\gamma^2)(-1+r^4\gamma^2) - \beta\left(1+\gamma^2(-3+r^4(1+\gamma^2))\right)\sqrt{k_0} + 2\Big(-2 + \sqrt{2}\Big)\left(2+\gamma^2(1+r^4(-1+2\gamma^2))\right)\lambda^4 k_0\Big)\Big) \Big/ \Bigg(r^3\left(-(-1+\gamma^2)^2-(-1+\gamma^4)\log\left(\frac{1}{\gamma}\right)+\beta\Big(2\gamma^2(-1 + \gamma^2)+(1+3\gamma^4)\log\left(\frac{1}{\gamma}\right)\Big)\sqrt{k_0} + \lambda^4\Big(-(-1+\gamma^2)\left(4-\sqrt{2}+\left(-8+7\sqrt{2}\right)\gamma^2\right)+2\left(-2+\sqrt{2}\right)(1 + \gamma^4)\log\left(\frac{1}{\gamma}\right)\Big)k_0 + 2\left(-1+\sqrt{2}\right)\beta\left(3-2\gamma^2+7\gamma^4\right)\lambda^4 k_0^{3/2}\Big)\Big)\Bigg), \tag{73}$$

$$\tau^{i}_{r\theta} = -\Bigg(\left(4\left(-1+\sqrt{2}\right) r^{-1+\sqrt{2}}\lambda^4 \sin[\theta]\left(1+2\gamma^2-3\gamma^4+\beta(3-2\gamma^2+7\gamma^4)\sqrt{k_0}\right)k_0\right) \Big/$$
$$\Bigg(-(-1+\gamma^2)^2-(-1+\gamma^4)\log\left(\frac{1}{\gamma}\right)+\beta\left(2\gamma^2(-1+\gamma^2)+(1+3\gamma^4)\log\left(\frac{1}{\gamma}\right)\right)\sqrt{k_0}$$
$$+\lambda^4\Bigg(-(-1+\gamma^2)\left(4-\sqrt{2}+\left(-8+7\sqrt{2}\right)\gamma^2\right)+2\left(-2+\sqrt{2}\right)(1+\gamma^4)\log\left(\frac{1}{\gamma}\right)\Bigg)k_0$$
$$+2\left(-1+\sqrt{2}\right)\beta(3-2\gamma^2+7\gamma^4)\lambda^4 k_0^{3/2}\Bigg)\Bigg), \tag{74}$$

$$\tau^{o}_{rr} = -\Bigg(\Big(2\lambda^2\cos[\theta]\Big((-1+\gamma^2)(-1+r^2(2+(2+r^2)\gamma^2))-\beta\Big(1+2r^2+(-3+r^4)\gamma^2+r^2(6$$
$$+r^2)\gamma^4\Big)\sqrt{k_0}+2\left(-2+\sqrt{2}\right)(-1+r)(1+r)(-2-(1+r^2)\gamma^2+2r^2\gamma^4)\lambda^4 k_0\Big)\Big) \Big/$$
$$\Bigg(r^3\Bigg(-(-1+\gamma^2)^2-(-1+\gamma^4)\log\left(\frac{1}{\gamma}\right)+\beta\left(2\gamma^2(-1+\gamma^2)+(1+3\gamma^4)\log\left(\frac{1}{\gamma}\right)\right)\sqrt{k_0}$$
$$+\lambda^4\Bigg(-(-1+\gamma^2)\left(4-\sqrt{2}+\left(-8+7\sqrt{2}\right)\gamma^2\right)+2\left(-2+\sqrt{2}\right)(1+\gamma^4)\log\left(\frac{1}{\gamma}\right)\Bigg)k_0$$
$$+2\left(-1+\sqrt{2}\right)\beta(3-2\gamma^2+7\gamma^4)\lambda^4 k_0^{3/2}\Bigg)\Bigg)\Bigg), \tag{75}$$

$$\tau^{i}_{rr} = -\Bigg(\left(2r^{-1+\sqrt{2}}\lambda^2\cos[\theta]\left(1+2\gamma^2-3\gamma^4+\beta(3-2\gamma^2+7\gamma^4)\sqrt{k_0}\right)\left(-1+2\left(-2+\sqrt{2}\right)\lambda^2 k_0\right)\right) \Big/$$
$$\Bigg(-(-1+\gamma^2)^2-(-1+\gamma^4)\log\left(\frac{1}{\gamma}\right)+\beta\left(2\gamma^2(-1+\gamma^2)+(1+3\gamma^4)\log\left(\frac{1}{\gamma}\right)\right)\sqrt{k_0}+\lambda^4\Bigg(-(-1$$
$$+\gamma^2)\left(4-\sqrt{2}+\left(-8+7\sqrt{2}\right)\gamma^2\right)+2\left(-2+\sqrt{2}\right)(1+\gamma^4)\log\left(\frac{1}{\gamma}\right)\Bigg)k_0$$
$$+2\left(-1+\sqrt{2}\right)\beta(3-2\gamma^2+7\gamma^4)\lambda^4 k_0^{3/2}\Bigg)\Bigg). \tag{76}$$

5 Results and discussion

In the present work, the author is interested to see the effect of permeability parameter k_0, the viscosity ratio of both regions, the particle volume fraction and discontinuity coefficient on the hydrodynamic drag force and the hydrodynamic permeability of a membrane built up by non-homogeneous porous cylindrical particles.

5.1 Effect of permeability parameter k_0

The variation of the dimensionless hydrodynamic permeability, L_{11} of a membrane with permeability parameter k_0 when $\beta = 0.5$, $\lambda = 0.3$, and $\gamma = 0.5$ for all models is shown in fig. 3. Figure 3 shows that the dimensionless hydrodynamic permeability, L_{11} of a membrane increases with increase of permeability parameter k_0 for all models. From this figure, it is also found that the dimensionless hydrodynamic permeability, L_{11} of a membrane is highest for Happel's model and lowest for Mehta-Morse's model.

The velocity profile outside the non-homogeneous porous region is decreased with increase of permeability parameter k_0 for all models when $\beta = 0.5$, $\lambda = 0.3$, $k_o = 0.3$, $\theta = \pi/4$ & $r = 0.5$ (fig. 4). It is also found that velocity is higher for Kuwabara's model for low values of permeability parameter k_0 but for high values of permeability parameter k_0, the value of velocity is higher for Mehta-Morse's model.

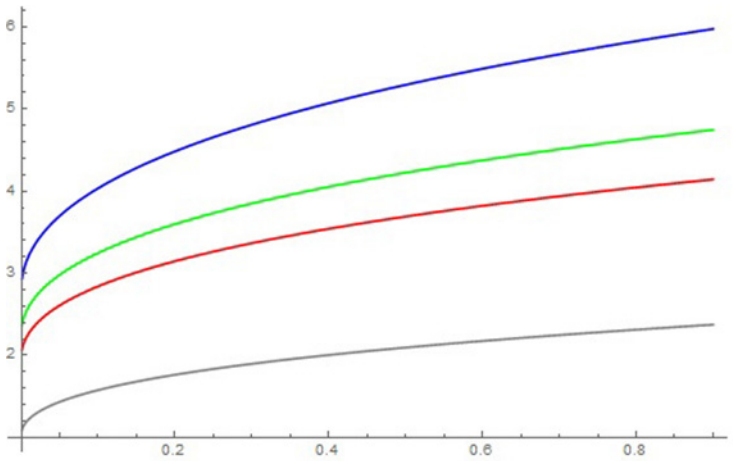

Fig. 3. Variation of the dimensionless hydrodynamic permeability of a membrane with permeability parameter k_0 for all models.

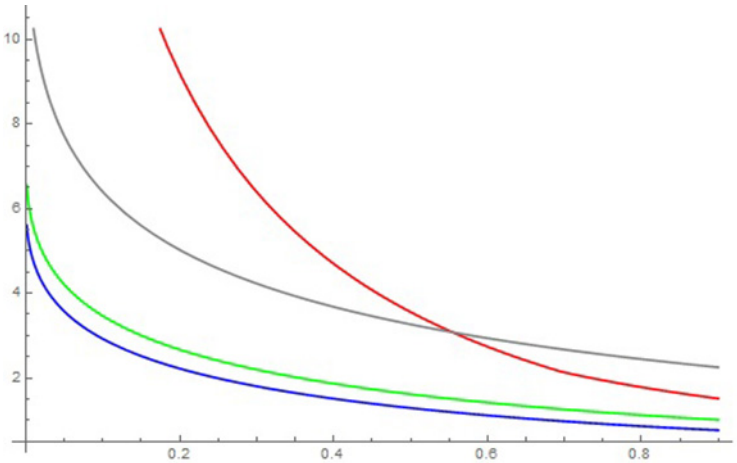

Fig. 4. Variation of velocity profile outside the non-homogeneous porous region with permeability parameter k_0 for all models.

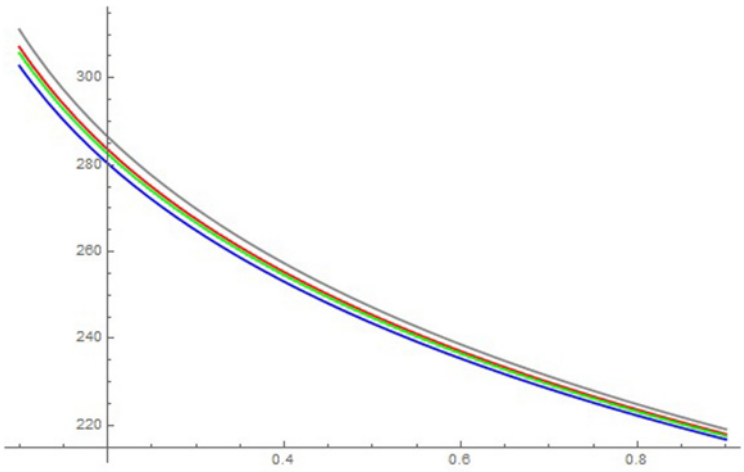

Fig. 5. Variation of normal stress outside the non-homogeneous porous region with permeability parameter k_0 for all models.

From figs. 5 and 6, the author observed that the normal and shear stresses outside the non-homogeneous porous medium decrease with increase of permeability parameter k_0 when $\beta = 0.5$, $\lambda = 5$, $k_o = 0.3$, $\theta = \pi/4$ & $r = 0.5$. It is also observed that the shear stress is higher than normal stress outside the non-homogeneous porous medium for all models.

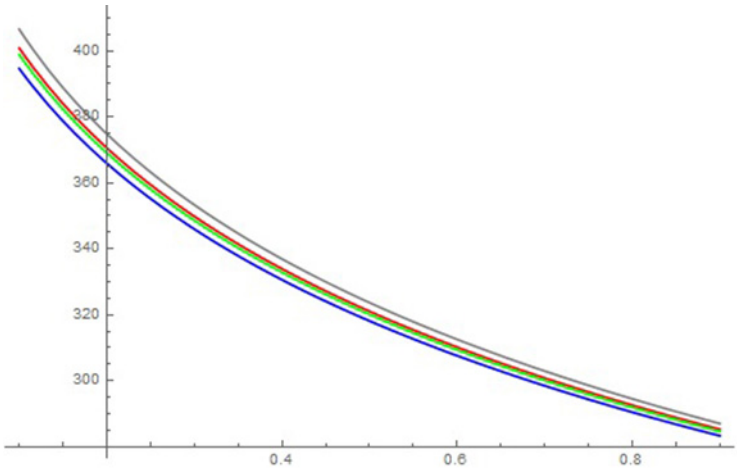

Fig. 6. Variation of shear stress outside the non-homogeneous porous region with permeability parameter k_0 for all models.

Table 1. Variation of normal and shearing stresses with permeability parameter.

		$k_o = 0.01$	$k_o = 0.03$	$k_o = 0.06$	$k_o = 0.09$	$k_o = 0.1$	$k_o = 0.3$	$k_o = 0.6$
Happel's model:	τ^o_{rr}	72.5454	101.325	105.661	104.987	104.514	94.2423	84.3421
$\lambda = 0.3$, $\gamma = 0.5$,	τ^i_{rr}	9.4168	4.4153	2.8987	2.3650	2.2568	1.6062	1.4554
$\beta = 0.5$, $r = 0.5$,	$\tau^o_{r\theta}$	65.178	120.800	131.98	133.062	132.843	121.895	109.601
$\theta = \pi/4$	$\tau^i_{r\theta}$	−0.6351	−0.7502	−0.7943	−0.8143	−0.8190	−0.8630	−0.8887
Kuwabara's model:	τ^o_{rr}	87.6579	108.545	109.96	108.169	107.458	95.5629	85.1049
$\lambda = 0.3$,	τ^i_{rr}	10.3028	4.6011	2.9759	2.4148	2.3017	1.6257	1.4694
$\gamma = 0.5$, $\beta = 0.5$,	$\tau^o_{r\theta}$	84.0407	130.584	137.95	137.529	136.989	123.822	110.756
$r = 0.5$, $\theta = \pi/4$,	$\tau^i_{r\theta}$	−0.6949	−0.7818	−0.8154	−0.8314	−0.8353	−0.8734	−0.8972
Kvashnin's model:	τ^o_{rr}	82.4963	106.159	108.555	107.133	106.5	95.1362	84.8591
$\lambda = 0.3$,	τ^i_{rr}	10.0002	4.5397	2.9507	2.3986	2.2871	1.6194	1.4649
$\gamma = 0.5$, $\beta = 0.5$,	$\tau^o_{r\theta}$	77.5983	127.355	136.0	136.075	135.641	123.199	110.384
$r = 0.5$, $\theta = \pi/4$	$\tau^i_{r\theta}$	−0.6744	−0.7714	−0.8049	−0.8258	−0.8300	−0.8700	−0.8944
Mehta-Morse's model:	τ^o_{rr}	103.945	115.578	114.02	111.138	110.199	96.7688	85.7959
$\lambda = 0.3$,	τ^i_{rr}	11.276	4.7820	3.0588	2.4612	2.3434	1.6436	1.4820
$\gamma = 0.5$, $\beta = 0.5$,	$\tau^o_{r\theta}$	104.369	140.103	143.543	141.697	140.848	125.581	111.803
$r = 0.5$, $\theta = \pi/4$	$\tau^i_{r\theta}$	−0.7593	−0.8126	−0.8354	−0.8474	−0.8505	−0.8830	−0.9050

During the analysis, it is found that normal and shear stresses inside the non-homogeneous porous region decrease with increase of permeability parameter k_0 for all models (table 1). From table 1, it is also concluded that the normal stress for Mehta-Morse's model is highest and lowest for Happel's model. The normal and shear stresses outside the non-homogeneous porous region is always greater than the normal and shear stresses inside the non-homogeneous porous region, respectively, for all models.

5.2 Effect of particle volume fraction

The effect of particle volume fraction γ on the dimensionless hydrodynamic permeability, L_{11} of a membrane, when $\beta = 0.5$, $\lambda = 0.3$, and $k_o = 0.3$ for all models is shown in fig. 7. Figure 7 shows that the dimensionless hydrodynamic permeability, L_{11} of a membrane, decreases with increase of particle volume fraction γ. It is also found that the rate of decrease of dimensionless hydrodynamic permeability L_{11} is higher for lower values of the particle volume fraction ($\gamma \leq 0.6$) and it becomes almost constant for higher values of the particle volume fraction ($\gamma > 0.6$).

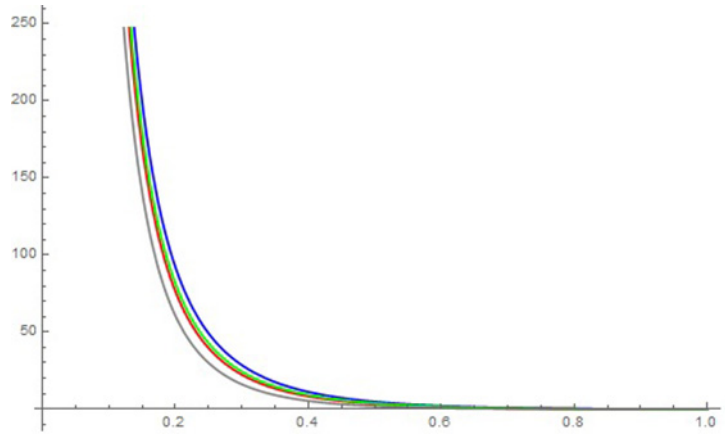

Fig. 7. Variation of the dimensionless hydrodynamic permeability of a membrane with particle volume fraction γ for all models.

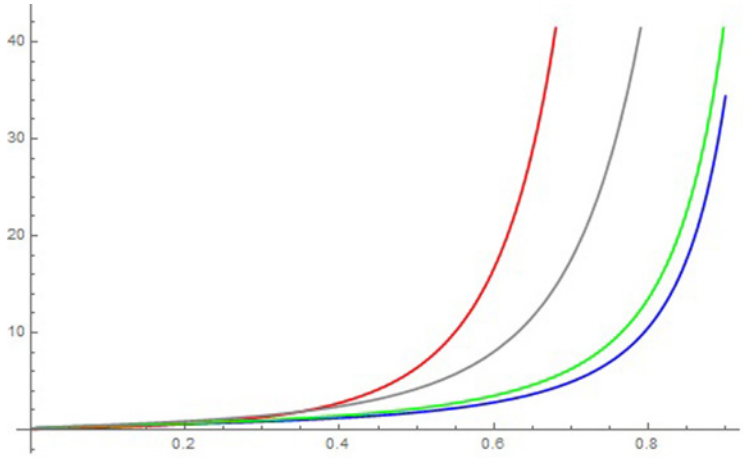

Fig. 8. Variation of velocity profile outside the non-homogeneous porous region with particle volume fraction γ for all models.

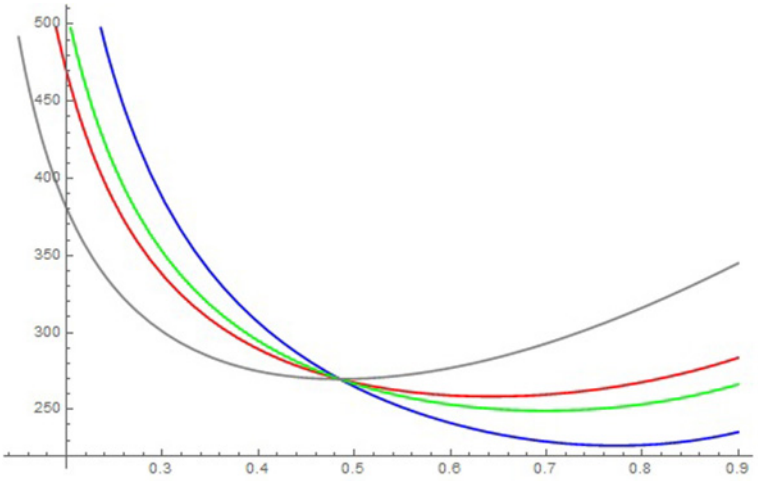

Fig. 9. Variation of normal stress outside the non-homogeneous porous region with particle volume fraction γ for all models.

From fig. 8, it is observed that the velocity profile outside the non-homogeneous porous region increases with increase of particle volume fraction γ for all models, when $\beta = 0.5$, $\lambda = 0.3$, $k_o = 0.3$, $\theta = \pi/4$ and $r = 0.5$ and the rate of increase is high for higher values of the particle volume fraction ($\gamma \geq 0.5$). Figures 9 and 10 show the variation of normal and shear stresses with particle volume fraction γ when $\beta = 0.5$, $\lambda = 5$, $k_o = 0.3$, $\theta = \pi/4$ & $r = 0.5$. From these figures, it is interesting to note that the normal and shear stresses decrease with increase of the particle volume fraction till $\gamma = 0.48$ but after $\gamma \geq 0.48$ the normal and shear stresses increase with increase of particle volume fraction γ.

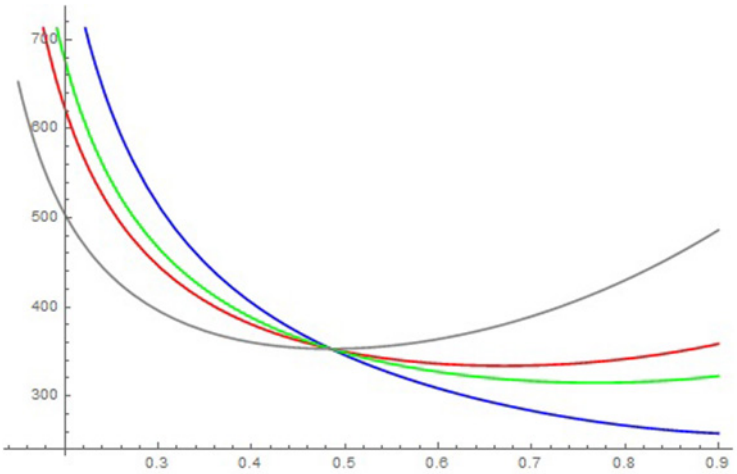

Fig. 10. Variation of shear stress outside the non-homogeneous porous region with particle volume fraction γ for all models.

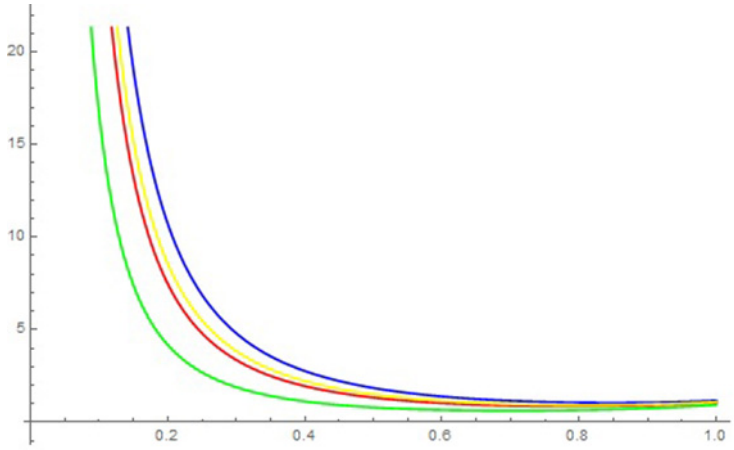

Fig. 11. Variation of the dimensionless hydrodynamic permeability of a membrane with viscosity ratio λ for all models.

It is also noticed from these figures that the value of normal and shear stresses is higher for Happel's model when particle volume fraction $\gamma \leq 0.48$ but when particle volume fraction $\gamma \geq 0.48$, then the value of normal and shear stresses is higher for Mehta-Morse's model.

5.3 Effect of viscosity ratio parameter λ

The dependence of dimensionless hydrodynamic permeability L_{11} of a membrane on the viscosity ratio λ, when $\beta = 0.5$, $\gamma = 0.5$, and $k_o = 0.3$ for all models is shown in fig. 11. From this figure, it is noticed that the dimensionless hydrodynamic permeability L_{11} of a membrane decreases with increase of viscosity ratio λ and variation in L_{11} becomes almost constant when $\lambda > 0.7$.

The effect of the viscosity ratio λ on the velocity profile outside the non-homogeneous porous region when $\beta = 0.5$, $\gamma = 0.5$, $k_o = 0.3$, $\theta = \pi/4$ and $r = 0.5$ for all models is discussed in fig. 12.

From this figure, it is observed that the velocity profile decreases with increase of viscosity ratio $\lambda \leq 0.9$ but it increases with increase of viscosity ratio $\lambda \geq 0.9$. The variation of normal and shear stresses outside the non-homogeneous porous region with viscosity ratio λ when, $\beta = 0.5$, $\gamma = 0.5$, $k_o = 0.3$, $\theta = \pi/4$ and $r = 0.5$ for all models are shown in figs. 13 and 14, respectively.

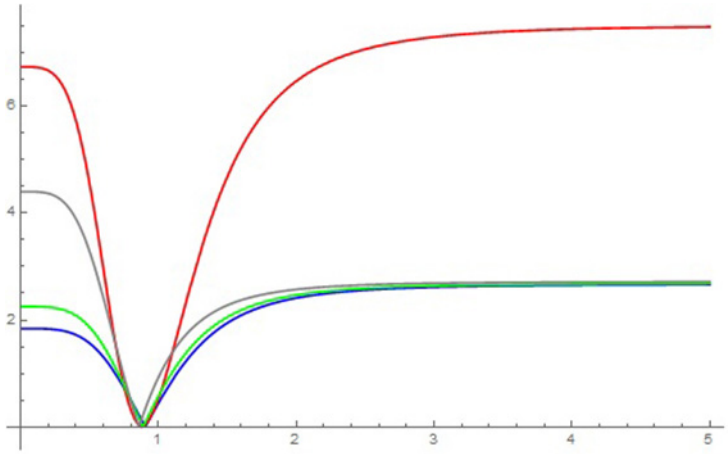

Fig. 12. Variation of velocity profile outside the non-homogeneous porous region with viscosity ratio λ for all models.

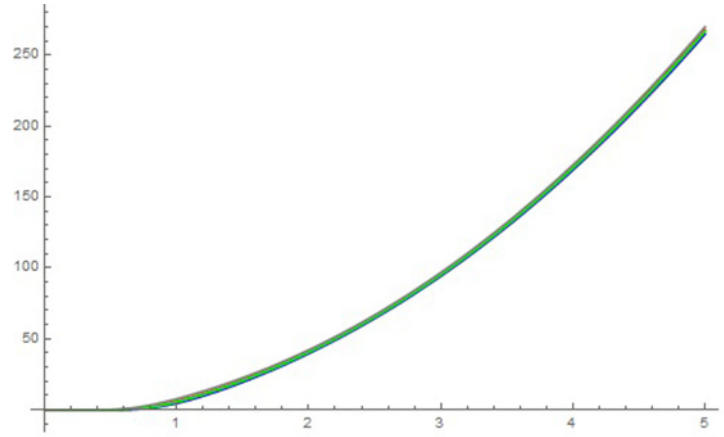

Fig. 13. Variation of normal stress outside the non-homogeneous porous region with viscosity ratio λ for all models.

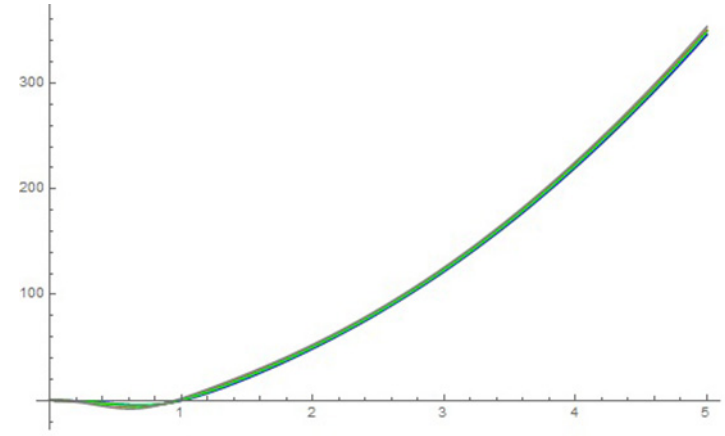

Fig. 14. Variation of shear stress outside the non-homogeneous porous region with viscosity ratio λ for all models.

These figures show that the variation in normal and shear stresses for all models is the same. Table 2 also shows the effect of viscosity ratio λ on the normal and shear stress outside and inside the non-homogeneous porous medium. From table 2, the author noticed that normal and shear stresses outside the non-homogeneous porous medium increase with increase of viscosity ratio λ for all models but normal and shear stresses inside the non-homogeneous porous medium increase with increase of viscosity ratio λ when the viscosity of the outer region is less than or equal to the viscosity of the non-homogeneous porous region and decreases with increase of viscosity ratio λ when the viscosity of the outer region is greater than the viscosity of the non-homogeneous porous region.

Table 2. Variation of normal and shearing stresses with viscosity ratio parameter.

		$\lambda = 0.1$	$\lambda = 0.5$	$\lambda = 1.0$	$\lambda = 5$	$\lambda = 10$
Happel's model: $\lambda = 0.3$, $\gamma = 0.5$, $\beta = 5$, $r = 0.5$, $\theta = \pi/4$	τ^o_{rr}	0.1234	2.9875	8.4539	71.3074	283.172
	τ^i_{rr}	0.0282	0.7338	2.2484	1.589	1.4704
	$\tau^o_{r\theta}$	0.0633	1.5560	5.2569	92.6823	370.16
	$\tau^i_{r\theta}$	−0.00007	−0.0419	−0.4135	−1.009	−1.0110
Kuwabara's model: $\lambda = 0.3$, $\gamma = 0.5$, $\beta = 5$, $r = 0.5$, $\theta = \pi/4$	τ^o_{rr}	−0.0169	3.3391	8.3262	70.7982	1871.36
	τ^i_{rr}	0.0561	1.0799	2.8057	1.5943	1.2802
	$\tau^o_{r\theta}$	−0.2064	1.0995	4.0578	92.1505	1402.49
	$\tau^i_{r\theta}$	−0.0001	−0.0617	−0.5160	−1.0121	−0.8802
Kvashnin's model: $\lambda = 0.3$, $\gamma = 0.5$, $\beta = 5$, $r = 0.5$, $\theta = \pi/4$	τ^o_{rr}	0.1334	3.1958	8.3732	70.9607	282.082
	τ^i_{rr}	0.0366	0.9389	2.6005	1.5926	1.4730
	$\tau^o_{r\theta}$	0.0522	1.2855	4.4994	92.3203	369.024
	$\tau^i_{r\theta}$	−0.0001	−0.0536	−0.4782	−0.1011	−1.0128
Mehta-Morse's model: $\lambda = 0.3$, $\gamma = 0.5$, $\beta = 5$, $r = 0.5$, $\theta = \pi/4$	τ^o_{rr}	0.1803	4.1129	8.1476	70.3489	280.161
	τ^i_{rr}	0.0758	1.8418	3.5849	1.5990	1.4776
	$\tau^o_{r\theta}$	−0.00001	0.0997	2.3811	91.6813	367.023
	$\tau^i_{r\theta}$	−0.0002	−0.1052	−0.6592	−0.1051	−1.0159

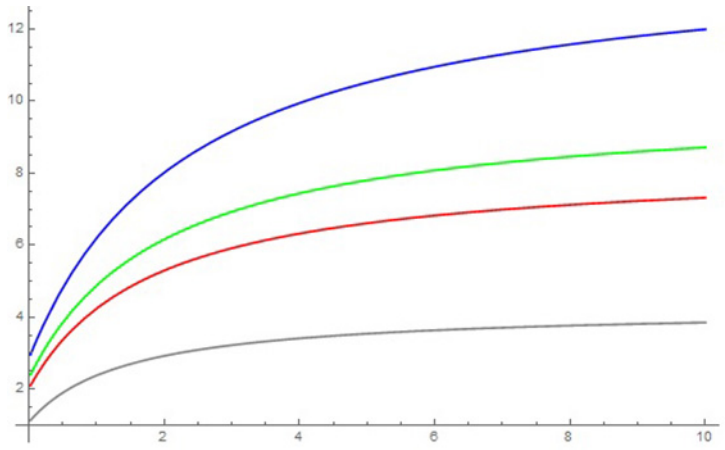

Fig. 15. Variation of the dimensionless hydrodynamic permeability of a membrane with discontinuity coefficient β for all models.

5.4 Effect of discontinuity coefficient β

The effect of discontinuity coefficient β on the dimensionless hydrodynamic permeability L_{11} of a membrane, when $\lambda = 0.3$, $\gamma = 0.5$, and $k_o = 0.3$ for all models is shown in fig. 15 and it is found that the dimensionless hydrodynamic permeability L_{11} of a membrane increases with increase of discontinuity coefficient β for all models.

It has been observed with this figure that the rate of increase in the dimensionless hydrodynamic permeability L_{11} of a membrane is faster for lower values of the discontinuity coefficient ($\beta < 3$) and for higher values, the variation in L_{11} becomes slow. The dependence of velocity profile outside the non-homogeneous porous on discontinuity coefficient β when $\lambda = 0.3$, $\gamma = 0.5$, $k_o = 0.3$, $\theta = \pi/4$ and $r = 0.5$ for all models is shown in fig. 16. From this figure, the author concluded that the velocity firstly decreases with increase of discontinuity coefficient when the values of β is low, a lower value of β is different for a different model (fig. 16) and then increases with increase of discontinuity coefficient β. The effects of discontinuity coefficient β on the normal and shear stresses outside the non-homogeneous porous region when $\lambda = 5$, $\gamma = 0.5$, $k_o = 0.3$, $\theta = \pi/4$ and $r = 0.5$ for all models are shown in figs. 17 and 18, respectively.

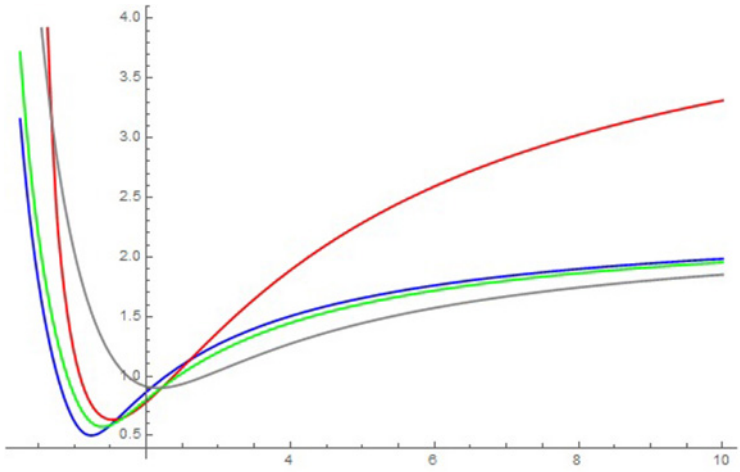

Fig. 16. Variation of velocity profile outside the non-homogeneous porous region with discontinuity coefficient β for all models.

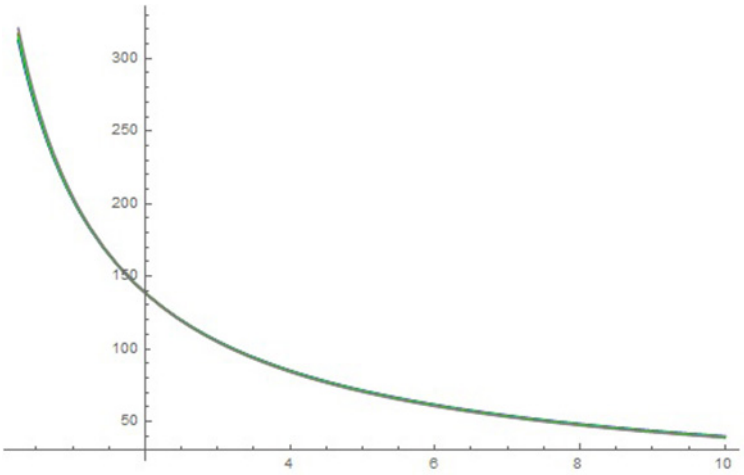

Fig. 17. Variation of normal stress outside the non-homogeneous porous region with discontinuity coefficient β for all models.

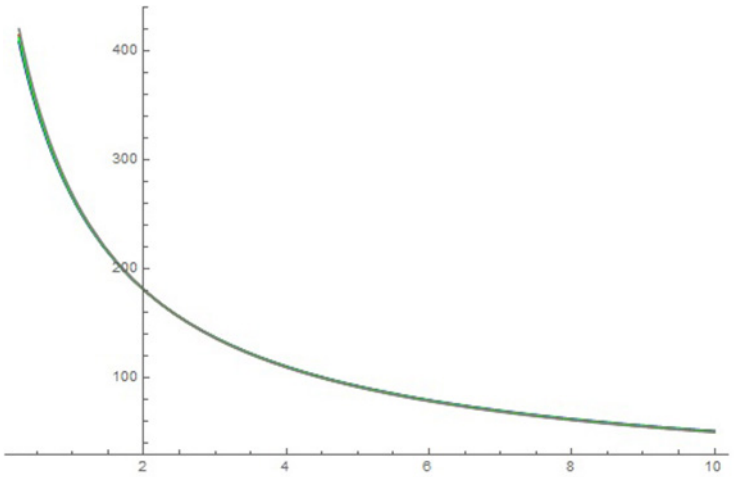

Fig. 18. Variation of shear stress outside the non-homogeneous porous region with discontinuity coefficient β for all models.

These figures show that the normal and shear stresses decrease rapidly with increase of discontinuity coefficient β for all models and become almost constant for higher values of discontinuity coefficient β.

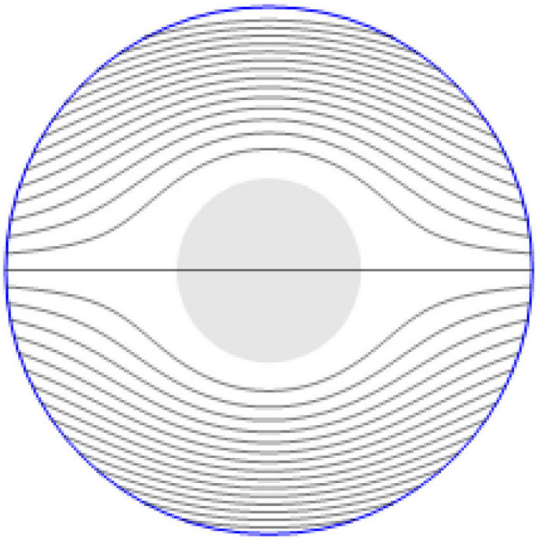

Fig. 19. Happel's model when $\lambda = 0.8$; $\beta = 0.3$; $k = 0.2$; $\gamma = 0.35$.

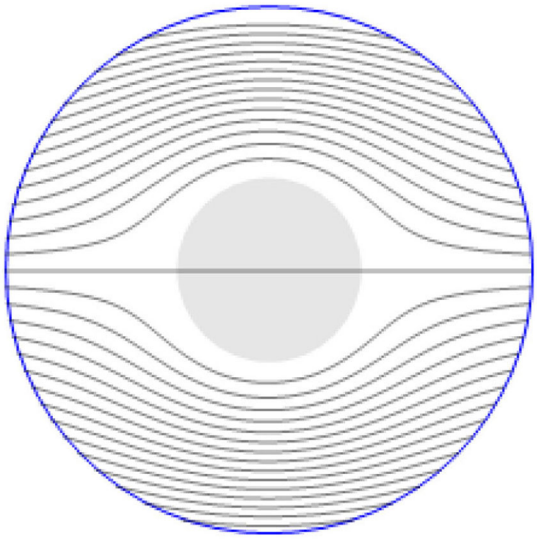

Fig. 20. Kuwabara's model when $\lambda = 0.8$; $\beta = 0.3$; $k = 0.2$; $\gamma = 0.35$.

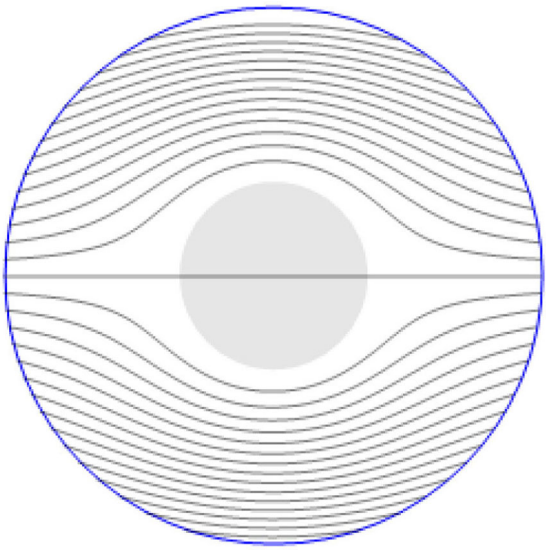

Fig. 21. Kvashnin's model when $\lambda = 0.8$; $\beta = 0.3$; $k = 0.2$; $\gamma = 0.35$.

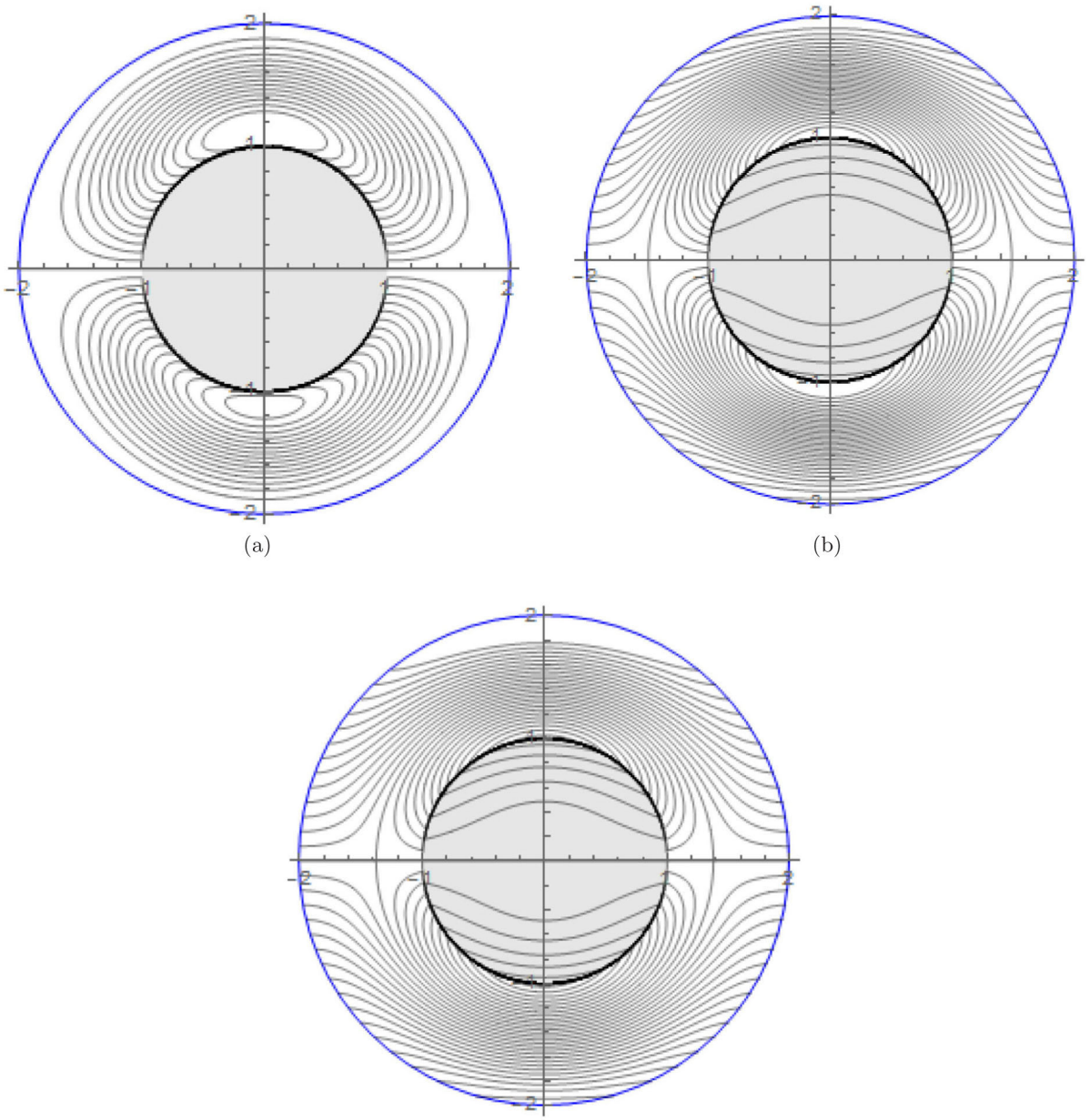

Fig. 22. (a) Mehta-Morse's model $\lambda = 0.7$; $\beta = 0.3$; $k = 0.1$; $\gamma = 0.5$. (b) Mehta-Morse's model when $\lambda = 0.7$; $\beta = 0.3$; $k = 0.5$; $\gamma = 0.5$. (c) Mehta-Morse's model when $\lambda = 0.7$; $\beta = 0.3$; $k = 0.9$; $\gamma = 0.5$.

5.5 Streamlines flow patterns

The streamlines flow patterns are shown in figs. 19–22. The effect of permeability parameter k_0 on the stream line flow pattern for Mehta-Morse's model is shown in fig. 22. On analyzing the effect of permeability parameter k_0 on the streamlines flow pattern, the author observed that the flow through the non-homogeneous porous region becomes easy with increase in permeability parameter k_0 and rotational tendency shifted towards the origin.

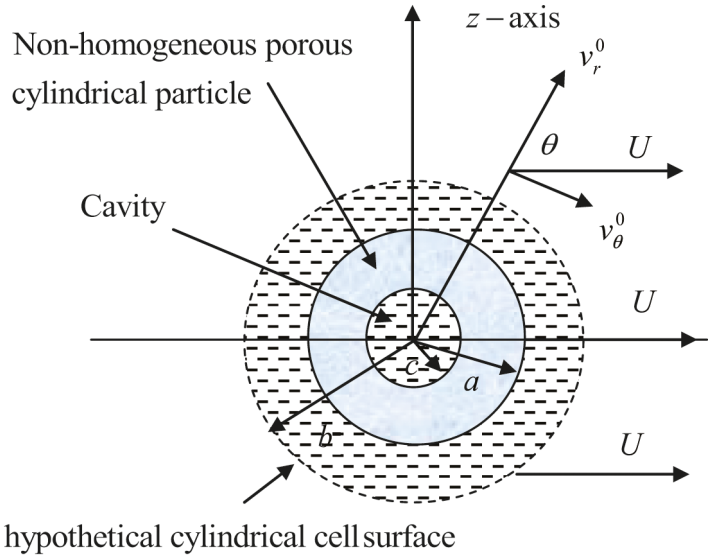

Fig. 23. Co-ordinate system when the membrane composed by cylindrical shell.

6 Comparative study of dimensionless hydrodynamic permeability of membrane composed by non-homogeneous porous cylindrical particles and cylindrical shell

Let us consider a membrane that is built up by a non-homogeneous porous cylindrical shell. The coordinate system of one particle of the membrane is shown in fig. 23. The flow outside the non-homogeneous porous cylindrical shell and inside the cavity with radius $\tilde{c}$ will be governed by the Stokes equation (3) together with the continuity condition (4) and the flow inside the non-homogeneous porous cylindrical shell will be governed by Darcy's equation (1) together with the continuity equation (2). Let $\psi^{(1)}$, $\psi^{(2)}$ and $\psi^{(3)}$ be the stream function formulation of the concerned equations outside the non-homogeneous porous cylindrical shell, inside the non-homogeneous porous cylindrical shell and inside the cavity respectively.

The stream function formulation of the concerned regions may be written as

$$\psi^{(1)}(r,\theta) = \left[B_1 r + B_2 r^3 + B_3/r + B_4 r \ln r\right] \sin\theta, \tag{77}$$

$$\psi^{(2)} = k_0 \lambda^2 \left[\left(1-\sqrt{2}\right) r^{1+\sqrt{2}} A_1 + \left(1+\sqrt{2}\right) r^{1-\sqrt{2}} A_2\right] \sin\theta, \tag{78}$$

$$\psi^{(3)}(r,\theta) = \left[C_1 r + C_2 r^3\right] \sin\theta, \tag{79}$$

where B_1, B_2, B_3, B_4, A_1, A_2, C_1 and C_2 are arbitrary constants which may be obtained by using suitable boundary conditions. The suitable boundary conditions for the considered case may be written as follows.

The suitable boundary conditions at the surface of cavity, *i.e.* at $r = \ell$, are

$$v_r^{(2)} = v_r^{(3)}, \qquad p^{(2)} = -p^{(3)} + 2\frac{\partial}{\partial r}\left(v_r^{(3)}\right), \qquad v_\theta^{(3)} - v_\theta^{(2)} = \beta\sqrt{k(r)}\frac{\partial v_\theta^{(3)}}{\partial r}. \tag{80}$$

The suitable boundary conditions at the surface of the non-homogeneous porous cylindrical shell, *i.e.* at $r = 1$, are

$$v_r^{(1)} = v_r^{(2)}, \qquad p^{(2)} = -p^{(1)} + 2\frac{\partial v_r^{(1)}}{\partial r}, \qquad v_\theta^{(1)} - v_\theta^{(2)} = \beta\sqrt{k(r)}\frac{\partial v_\theta^{(1)}}{\partial r}. \tag{81}$$

The suitable boundary conditions at the surface of the hypothetical cell, *i.e.* at $r = \frac{1}{\gamma_1}$, are

i) The condition of uniform velocity at the hypothetical cell surface, *i.e.*,

$$v_r^{(1)} = \cos\theta. \tag{82}$$

ii) *According to Happel's model*:

$$\tau_{r\theta}^{(1)}(m,\theta) = 0. \tag{83a}$$

Table 3. Comparison of dimensionless hydrodynamic permeability of a membrane built up by cylindrical particles and cylindrical shell enclosing a cavity.

		$k_o = 0.01$	$k_o = 0.03$	$k_o = 0.06$	$k_o = 0.09$	$k_o = 0.1$	$k_o = 0.3$	$k_o = 0.6$
Happel's model:								
$\lambda = 0.3$, $\gamma = 0.5$,	L_{11}^{*}	3.2177	3.5067	3.7775	3.9776	4.0354	4.8085	5.4898
$\beta = 0.5$, $\ell = 0.5$	L_{11}^{**}	0.0077	0.0118	0.0168	0.0213	0.0227	0.0456	0.0566
Kuwabara's model:								
$\lambda = 0.3$, $\gamma = 0.5$,	L_{11}^{*}	2.2716	2.4751	2.6637	2.8019	2.8416	3.3661	3.8209
$\beta = 0.5$, $\ell = 0.5$	L_{11}^{**}	0.0061	0.0095	0.0138	0.0177	0.0190	0.0384	0.0409
Kvashnin's model:								
$\lambda = 0.3$, $\gamma = 0.5$,	L_{11}^{*}	2.5974	2.8286	3.0436	3.2015	3.2500	3.8497	4.3746
$\beta = 0.5$, $\ell = 0.5$	L_{11}^{**}	0.0067	0.0104	0.0150	0.0191	0.0204	0.0409	0.0460
Mehta-Morse's model:								
$\lambda = 0.3$, $\gamma = 0.5$,	L_{11}^{*}	1.2246	1.3518	1.4685	1.5535	1.5778	1.8977	2.1755
$\beta = 0.5$, $\ell = 0.5$	L_{11}^{**}	0.0027	0.0053	0.0084	0.1220	0.0133	0.0312	0.0261

iii) *According to Kuwabara's model*:

$$\nabla^2 \psi^{(1)}(m, \theta) = 0. \tag{83b}$$

iv) *According to Kvashnin's model*:

$$\frac{\partial v_\theta^{(1)}}{\partial r} = 0. \tag{83c}$$

v) *According to Mehta-Morse's model*:

$$v_\theta^{(1)} = -\sin\theta, \tag{83d}$$

where the symbols having their own meaning and superscript (1), (2) and (3) show the respective regions. Here, $\ell = \frac{\tilde{c}}{\tilde{a}}$ and $\gamma_1^3 = \frac{(\tilde{b}-\tilde{a})^3}{\tilde{b}^3}$. By using these boundary conditions, one can find all the constants for all the models and hence, one can evaluate the dimensionless hydrodynamic permeability of the membrane composed by a non-homogeneous porous cylindrical shell by using eq. (55). Table 3 shows the comparative study of dimensionless hydrodynamic permeability of a membrane built up by non-homogeneous porous cylindrical particles and a non-homogeneous porous cylindrical shell enclosing a cavity.

$L_{11}^{*} \rightarrow$ Dimensionless hydrodynamic permeability of a membrane composed by non-homogeneous porous cylindrical particles.

$L_{11}^{**} \rightarrow$ Dimensionless hydrodynamic permeability of a membrane composed by a non-homogeneous porous cylindrical shell.

From table 3, it is concluded that the nature of variation in the dimensionless hydrodynamic permeability of a membrane composed by non-homogeneous porous cylindrical particles and a cylindrical shell enclosing a cavity is the same and in both cases, the dimensionless hydrodynamic permeability of the membrane increases with increase of permeability parameter k_0. From this table, it is also noticed that the dimensionless hydrodynamic permeability of the membrane is very small when the membrane is composed of a non-homogeneous porous cylindrical shell enclosing a cavity. This table also gives the information of which model is more suitable for the physical problem.

7 Conclusions

In the present work the author has discussed the dependence of hydrodynamic permeability L_{11}, the velocity profile and stresses of a membrane built up by non-homogeneous porous cylindrical particles on viscosity ratio λ of a fluid and non-homogeneous porous medium, permeability parameter k_0 of the non-homogeneous porous region, discontinuity coefficient β and particle volume fraction γ graphically. On analyzing the effect of permeability parameter k_0, the author found that the permeability parameter plays an important role in controlling the hydrodynamic drag force and hydrodynamic permeability. During the analysis, it is also observed that the viscosity ratio is also another important controlling parameter for the hydrodynamic drag force and hydrodynamic permeability. The outcomes of this research may be useful in further applications where the movement of fluid is through a non-homogeneous region. The findings may be used in the contaminant clean-up, filtration and water purification processes under the considered situations.

The author is thankful to Science & Engineering Research Board, Government of India for supporting this research work under the research grant No. SR/ FTP/ MS-47/ 2012.

Nomenclature

a	Radius of non-homogeneous porous cylindrical particle	λ	Viscosity ratio
		$\tilde{L}_{11}$	Dimensional hydrodynamic permeability
b	Radius of hypothetical cell	L_{11}	Non-dimensional hydrodynamic permeability
c	Radius of cavity	$\tilde{K}(r)$	Permeability coefficient of the non-homogeneous porous region
(r, θ, z)	Cylindrical polar co-ordinates		
v_r, v_θ	Velocity components of fluid at any point	μ	Viscosity of the medium
		β	Dimensionless discontinuity constant
p	Fluid pressure at any point	L_{11}^*	Dimensional hydrodynamic permeability of the membrane composed of non-homogeneous porous cylindrical particles
τ_{rr}	Normal stress		
$\tau_{r\theta}$	Tangential stress		
U	Uniform velocity of fluid	L_{11}^{**}	Dimensional hydrodynamic permeability of the membrane composed of non-homogeneous porous cylindrical shell enclosed in a cavity
k_o	Permeability parameter		
F	Hydrodynamic drag force		
γ	Particle volume fraction	$\ell = \frac{\tilde{c}}{\tilde{a}}$	Dimensionless quantity
ψ	Stream function		

References

1. G.G. Stokes, *On the Theories of the Internal Friction of Fluids in Motion, and of the Equilibrium and Motion of Elastic Bodies* (Cambridge Philosophical Society, 1851).
2. H.P.G. Darcy, *Les fontaines publiques de la ville de Dijon Paris* (Victor Dalmont, 1856).
3. D.D. Joseph, L.N. Tao, Z. Angew. Math. Mech. **44**, 361 (1964).
4. D.A. Nield, A. Bejan, *Convection in Porous Media* (Springer, New York, 1999).
5. L. Preziosi, A. Farina, Int. J. Non-Linear Mech. **37**, 485 (2002).
6. G.S. Beavers, D.D. Joseph, J. Fluid Mech. **30**, 197 (1967).
7. I.P. Jones, Proc. Camb. Philos. Soc. **73**, 231 (1973).
8. J. Masliyah, G. Neale, K. Malysa, T.V. de Ven, Chem. Eng. Sci. **4**, 245 (1987).
9. Y. Qin, P.N. Kaloni, Z. Angew. Math. Mech. **73**, 77 (1993).
10. W.W. Hackborn, Can. Appl. Math. Quart. **8**, 171 (2000).
11. I.B. Stechkina, Fluid Dyn. **14**, 912 (1979).
12. I. Pop, P. Cheng, Int. J. Eng. Sci. **30**, 257 (1992).
13. M.P. Singh, J.L. Gupta, Z. Angew. Math. Mech. **54**, 17 (1971).
14. S. Deo, Sadhana **29**, 381 (2004).
15. M. Ellero, M. Kroger, S. Hess, J. Non-Newtonian Fluid Mech. **105**, 35 (2002).
16. A.S. Kim, R. Yuan, J. Membr. Sci. **249**, 89 (2005).
17. E.I. Saad, Meccanica **48**, 1747 (2013).
18. D. Palaniappan, K. Archana, S.K. Khan, Z. Angew. Math. Mech. **77**, 791 (1997).
19. S.M. Datta, Shukla, Cal. Math. Soc. **95**, 63 (2003).
20. P.D. Verma, B.S. Bhatt, J. Pure Appl. Math. **15**, 908 (1976).
21. S. Whitaker, Transp. Porous Media **1**, 3 (1986).
22. F.R. Mandujano, F. Peralta, Rev. Mex. Fis. **51**, 87 (2005).
23. S. Deo, P.K. Yadav, Int. J. Math. Math. Sci. **2008**, 651910 (2008).
24. N.S. Cheng, Z.Y. Hao, S.K. Tan, Exp. Therm. Fluid Sci. **32**, 1538 (2008).
25. S. Deo, P.K. Yadav, A. Tiwari, Appl. Math. Mod. **34**, 1329 (2010).
26. S. Deo, A.N. Filippov, A. Tiwari, S.I. Vasin, V. Starov, Adv. Colloid Interface Sci. **164**, 21 (2011).
27. J. Prakash, G.P. Raja Sekhar, Meccanica **47**, 1079 (2012).
28. O.V. Grigoreva, Sh.Kh. Zaripov, Russ. Aeronaut. **55**, 19 (2012).
29. P.K. Yadav, S. Deo, Meccanica **47**, 1499 (2012).
30. P.K. Yadav, Meccanica **48**, 1607 (2013).
31. M.S. Valipour, S. Rashidi, M. Bovand, R. Masoodi, Eur. J. Mech. **46**, 74 (2014).

32. A. Barletta, L. Storesletten, Int. J. Therm. Sci. **97**, 9 (2015).
33. S. Srinivasan, K.R. Rajagopal, Int. J. Non-Linear Mech. **78**, 112 (2016).
34. B.R. Jaiswal, B.R. Gupta, Meccanica **52**, 69 (2017).
35. E.I. Saad, Meccanica **47**, 2055 (2012).
36. I.V. Chernyshev, Fluid Dyn. **35**, 147 (2000).
37. J. Happel, H. Brenner, *Low Reynolds Number Hydrodynamics* (Prentice-Hall Inc., UK, 1965) chapt. 4.
38. S.I. Vasin, A.N. Filippov, V.M. Starov, Adv. Coll. Interface Sci. **139**, 83 (2008).